1521-009X/46/6/888–896$35.00
Drug Metabolism and Disposition

https://doi.org/10.1124/dmd.118.080952
Drug Metab Dispos 46:888–896, June 2018

Hepatic Abundance and Activity of Androgen- and Drug-Metabolizing Enzyme UGT2B17 Are Associated with Genotype, Age, and Sex[S]

Deepak Kumar Bhatt, Abdul Basit, Haeyoung Zhang, Andrea Gaedigk, Seung-been Lee, Katrina G. Claw, Aanchal Mehrotra, Amarjit Singh Chaudhry, Robin E. Pearce, Roger Gaedigk, Ulrich Broeckel, Timothy A. Thornton, Deborah A. Nickerson, Erin G. Schuetz, John K. Amory, J. Steven Leeder, and Bhagwat Prasad

Departments of Pharmaceutics (D.K.B., A.B., H.Z., K.G.C., A.M., B.P.), Genome Sciences (S.L., D.A.N.), Biostatistics (T.A.T.), and Medicine (J.K.A.), University of Washington, Seattle, Washington; Division of Pediatric Pharmacology and Medical Toxicology, Department of Pediatrics, Children's Mercy Hospitals and Clinics, Kansas City, Missouri (A.G., R.E.P., R.G., J.S.L.); Department of Pharmaceutical Sciences, St. Jude Children's Research Hospital, Memphis, Tennessee (A.S.C., E.G.S.); and Section of Genomic Pediatrics, Department of Pediatrics, and Human and Molecular Genetics Center, Medical College of Wisconsin, Milwaukee, Wisconsin (U.B.)

Received February 13, 2018; accepted March 29, 2018

ABSTRACT

The major objective of this study was to investigate the association of genetic and nongenetic factors with variability in protein abundance and in vitro activity of the androgen-metabolizing enzyme UGT2B17 in human liver microsomes (n = 455). UGT2B17 abundance was quantified by liquid chromatography-tandem mass spectrometry proteomics, and enzyme activity was determined by using testosterone and dihydrotestosterone as in vitro probe substrates. Genotyping or gene resequencing and mRNA expression were also evaluated. Multivariate analysis was used to test the association of UGT2B17 copy number variation, single nucleotide polymorphisms (SNPs), age, and sex with its mRNA expression, abundance, and activity. UGT2B17 gene copy number and SNPs (rs7436962, rs9996186, rs28374627, and rs4860305) were associated with gene expression, protein levels, and androgen glucuronidation rates in a gene dose-dependent manner. UGT2B17 protein (mean ± S.D. picomoles per milligram of microsomal protein) is sparsely expressed in children younger than 9 years (0.12 ± 0.24 years) but profoundly increases from age 9 years to adults (~10-fold) with ~2.6-fold greater abundance in males than in females (1.2 vs. 0.47). Association of androgen glucuronidation with UGT2B15 abundance was observed only in the low UGT2B17 expressers. These data can be used to predict variability in the metabolism of UGT2B17 substrates. Drug companies should include UGT2B17 in early phenotyping assays during drug discovery to avoid late clinical failures.

Introduction

Uridine 5′-diphospho-glucuronosyltransferases (UGTs; EC 2.4.1.17) facilitate excretion of a wide variety of lipophilic drugs, environmental chemicals, and endogenous substrates containing hydroxyl, carboxyl, amino, and sulfur-containing functional groups by catalyzing conjugation of these substrates with glucuronic acid to increase hydrophilicity. UGT enzymes belong to distinct subfamilies of more than 26 genes with 19 well characterized functional proteins. The functional isoforms belong to the UGT1 and UGT2 superfamilies, which are further divided into three subfamilies, based on their sequence similarities, into UGT1As (UGT1A1, UGT1A3–UGT1A10), UGT2As (UGT2A1–UGT2A3), and UGT2Bs (UGT2B4, UGT2B7, UGT2B10, UGT2B11, UGT2B15, UGT2B17, and UGT2B28) (Guillemette, 2003; Oda et al., 2015; Yuan et al., 2016).

Although all hepatic UGT isoforms are generally variable, UGT2B17 shows extensively greater interindividual variability in its protein abundance and activity (Fallon et al., 2013; Neumann et al., 2016), and it is expressed in a variety of tissues, such as liver, intestine, kidney, testis, uterus, placenta, mammary gland, adrenal gland, skin, and prostate (Beaulieu et al., 1996; Ekstrom et al., 2013). Numerous endogenous steroids, including testosterone (T), dihydrotestosterone (DHT), androstane-3-α, 17-β-diol (3-α-diol), androsterone and estradiol, and xenobiotics (e.g., 17-dihydroexemestane, vorinostat, lorcaserin) have been identified as substrates of UGT2B17

Most of this work was supported by the National Institute of Child Health and Human Development (NICHD), National Institutes of Health (NIH) grant [R01 HD081299]. The data collection was also supported by NIH grants, [U01 GM092676] and [P01 GM116691]. The NICHD Brain and Tissue Bank for Developmental Disorders at the University of Maryland is funded by the NIH contract, [N01-HD-9-0011/HHSN275200900011C] and the Liver Tissue Cell Distribution System is funded by NIH contract number, [N01-DK-7-0004/HHSN267200700004C].

https://doi.org/10.1124/dmd.118.080952.

[S]This article has supplemental material available at dmd.aspetjournals.org.

ABBREVIATIONS: BSA, bovine serum albumin; CNV, copy number variation; DHT, dihydrotestosterone; FPKM, fragments per kilobase per million reads; HLM, human liver microsome; HSA, human serum albumin; LC-MS/MS, liquid chromatography-tandem mass spectrometry; LD, linkage disequilibrium; LLOQ, lower limit of quantification; LOD, limit of detection; PK, pharmacokinetics; P450, cytochrome P450 enzyme; PGRN, Pharmacogenomics Research Network; SNPs, single nucleotide polymorphisms; T, testosterone; UGT, uridine 5′-diphospho-glucuronosyltransferases.

(Beaulieu et al., 1996; Wong et al., 2011; Sadeque et al., 2012; Chen et al., 2016b; Neumann et al., 2016). The expression of UGT2B17 in sex hormone–sensitive organs also indicates its role in sex hormone homeostasis. For example, although controversial, gene deletion in UGT2B17 is associated with greater risk of developing androgen-sensitive prostate diseases (Barbier and Belanger, 2008; Paquet et al., 2012; Kpoghomou et al., 2013; Gauthier-Landry et al., 2015). The *UGT2B17* gene-deletion allele has been shown to be associated with several other pathophysiological conditions, such as obesity (Zhu et al., 2015), chronic lymphocytic leukemia (Gruber et al., 2013), and endometrial cancer (Hirata et al., 2010). UGT2B17 also appears to play a critical role in the metabolism of tobacco-specific carcinogens and the risk of lung cancer (Lazarus et al., 2005; Chen et al., 2016a). In addition, high intratumoral UGT2B17 expression levels correlate with better survival outcomes in patients with breast cancer (Hu et al., 2016). Besides its role in disease pathophysiology, the *UGT2B17* gene deletion is associated with false-negative doping test results, which in turn is linked to variable testosterone metabolism (Schulze et al., 2008). An investigational drug developed by Merck, MK-7246, a selective CRTH2 (prostaglandin D2 receptor 2) antagonist, was discontinued from development after unpredicted variability observed in its pharmacokinetics (PK). MK-7246 was later characterized as a selective UGT2B17 substrate (Wang et al., 2012). Similarly, the PK and anticancer effectiveness of UGT2B17 substrates 17-dihydroexemestane and vorinostat are highly variable (Wong et al., 2011; Chen et al., 2016b). Particularly, the normalized 17-dihydroexemestane and vorinostat levels were 28% and 26% higher, respectively, in subjects carrying the UGT2B17 gene deletion compared with those carrying the reference allele (Wong et al., 2011; Luo et al., 2017). The in vitro glucuronidation rate of 17-dihydroexemestane is significantly decreased (14-fold) in human liver microsomes (HLMs) exhibiting the UGT2B17 deletion genotype versus wild-type UGT2B17 HLMs (Sun et al., 2010). Taken together, high variability in UGT2B17 abundance significantly contributes to an unpredictable fate of its substrates that may lead to adverse pathophysiologic consequences and drug toxicity or lack of efficacy.

To understand more completely the underlying causes of UGT2B17 variability, we investigated the association of genetic and nongenetic factors with variability in protein abundance and in vitro activity of UGT2B17 in HLMs. The knowledge of individual contribution of population factors in UGT2B17 variability can be applied to the prediction of the metabolism of androgens and other UGT2B17 substrates. Further, because androgens are also metabolized by UGT2B15 (minor pathway), we studied the effect of its genetic polymorphism (UGT2B15*2) on the metabolism of testosterone and DHT, particularly in the poor expressers of UGT2B17.

Materials and Methods

Chemicals and Reagents. Iodoacetamide, dithiothreitol, and Pierce trypsin protease (MS grade) were purchased from Thermo Fisher Scientific (Rockford, IL). Ammonium bicarbonate buffer (98% purity) was purchased from Acros Organics (Geel, Belgium). Chloroform, MS-grade acetonitrile, methanol, and formic acid were purchased from Fischer Scientific (Fair Lawn, NJ). Human serum albumin (HSA) and bovine serum albumin (BSA) were obtained from Calbiochem (Billerica, MA) and Thermo Fisher Scientific, respectively. The purified light peptides were purchased from New England Peptides (Cambridge, MA). Synthetic isotopically pure heavy stable isotope-labeled peptides were produced by Thermo Fisher Scientific. UDPGA and $MgCl_2$ were purchased from Sigma-Aldrich (St. Louis, MO). Tesosterone (1 mg/ml in 100% acetonitrile) and testosterone-glucuronide were purchased from Cerilliant (Round Rock, TX). Testosterone-glucuronide was dissolved in 100% methanol (1 mg/ml). DHT (1 mg/ml in methanol) and DHT-glucuronide were purchased from Sigma-Aldrich and Cerilliant, respectively. Testosterone-glucuronide-d3 and DHT-glucuronide were procured from Cerilliant.

Human Liver Tissue and Preparation of Microsomes. Previously prepared HLM samples (Pearce et al., 2016; Shirasaka et al., 2016) were used in this study. The liver tissue samples for HLM preparation were received from three liver tissue banks: 1) the University of Washington Human Liver Bank (Seattle, WA) ($n = 56$), 2) Children's Mercy Kansas City (Kansas City, MO) ($n = 128$), and 3) the Liver Bank at the St. Jude Children's Research Hospital (Memphis, TN) ($n = 271$). The Children's Mercy Kansas City samples were originally obtained from the University of Maryland Brain and Tissue Bank for Developmental Disorders and the Liver Tissue Cell Distribution System. Additional details on the selection, procurement, and storage of the livers and investigator blinding for sample analyses have been described previously (Prasad et al., 2014; Shirasaka et al., 2016; Tanner et al., 2017). Age, sex, and ethnicity were known for 96%, 98%, and 88% of the liver donors, respectively (Supplemental Table S1). The age range for donors was from 0 to 87 years (median age, 24 years). Of the 455 samples analyzed for UGT2B abundance, demographic association analyses were conducted on 423 samples for which *UGT2B17* copy number variation (CNV) information was available. Sex distribution of these 423 samples was 252 males, 163 females, and eight unknown. The ethnicity distribution was 333 Caucasian, 26 African American, four Hispanic, one Native American, one Asian, one Pacific Islander, and 56 unknown. Cause of death, medications used, and liver pathology were known for less than 50% of the donors. The collection and use of these tissues for research purposes were approved by the human subjects Institutional Review Boards of the University of Washington (Seattle, WA), the St. Jude Children's Research Hospital (Memphis, TN), and the Pediatric Institutional Review Board of Children's Mercy Kansas City (Kansas City, MO).

UGT2B17 and UGT2B15 Protein Quantification in HLM Samples. Total protein quantification in HLM samples was performed using a bicinchonic acid assay kit (BCA Protein Assay Kit; Pierce Biotechnology, Waltham, MA). HLMs (80 μl, 2 mg/ml total protein) were digested as described in the Supplemental Materials. The surrogate peptides of UGT2B17 (FSVGYTVEK and SVINDPIYK) and UGT2B15 (SVINDPVYK) were quantified in the digested samples using a validated liquid chromatography-tandem mass spectrometry (LC-MS/MS) method (Vrana et al., 2017), described in the Supplemental Materials.

***UGT2B17* mRNA Quantification.** A subset of liver tissue samples ($n = 230$) were available for *UGT2B17* mRNA expression analysis (Supplemental Table S1). Details of the RNA-seq procedures, including RNA isolation, TruSeq-stranded mRNA preparation, and read processing and analysis pipeline have been described previously (Tanner et al., 2017). mRNA transcript levels are presented in fragments per kilobase per million reads (FPKM) values.

***UGT2B17* Sequencing, Genotyping, Haplotype and Copy Number Variation Analysis.** Because liver samples were obtained from different sources, two approaches, gene sequencing and genotyping, were used for genetic characterization of the liver tissue samples, as discussed in the Supplemental Materials. The University of Washington and St. Jude Liver Bank samples were sequenced using the Pharmacogenomics Research Network (PGRN)-Seq platform, a targeted sequencing approach, as described elsewhere (Gordon et al., 2016), whereas the samples provided by Children's Mercy were genotyped on DMET or PharmacoScan arrays (Affymetrix, Santa Clara, CA). Linkage disequilibrium (LD) analysis of *UGT2B17* variants and inferred haplotypes were determined using Haploview 4.2 (Cambridge, MA).

UGT2B17 and UGT2B15 Enzyme Activity Assay. For activity assays, 346 HLM samples (donor age ranges from 0 to 87 years; median age = 18 years, Supplemental Table S1) were available. Glucuronidation activity was determined by quantifying the rates of testosterone- and DHT-glucuronide formation (picomoles per minute per milligram of microsomal protein) in triplicate. The assay reactions contained 0.1 mg/ml HLM protein, 0.1 M phosphate buffer (pH 7.4), a mix of 1 μM testosterone and 1 μM DHT, BSA (0.01%), and alamethicin (0.1 mg/ml) (final volume of 95 μl). Final vehicle (methanol or ethanol) concentration was less than 1%. Reactions were preincubated for 15 minutes on ice. UDPGA (5 μl; final concentration, 2.5 mM) was added to initiate reactions, and mixtures were gently agitated for 30 minutes at 37°C before being quenched with ice-cold acetonitrile containing 50 ng/ml progesterone (200 μl, internal standard) and subjected to centrifugation for 5 minutes at ~1300*g*. Supernatants were analyzed by an optimized LC-MS/MS method provided in the Supplemental Materials.

Data Analysis. We used a robust strategy to ensure optimum reproducibility of UGT2B17 and UGT2B15 protein quantification (Bhatt and Prasad, 2018). For example, ion suppression was addressed by using heavy peptide internal standards. BSA or HSA was used as an exogenous protein internal standard, which was added to each sample in a fixed quantity before desalting by methanol-chloroform-water extraction and trypsin digestion. The addition of BSA or HSA addresses the variability introduced during predigestion processing, such as 1) protein loss during methanol-chloroform-water extraction and 2) sample-to-sample trypsin digestion artifacts. To address interbatch variability, two to three sets of pooled representative HLM samples were processed each day, which served as quality controls across the entire study. In total, a three-step data normalization approach was used; first, average light peak areas for specific peptide daughter fragments were divided by corresponding average heavy peak areas. Next, this ratio was further divided by the BSA or HSA light/heavy area ratio. Finally, for each day, these data were further normalized by mean values of the quality control values run with each individual batch to adjust for any interday variability.

Ontogeny was measured by categorical and continuous analyses of age versus UGT2B17 protein abundance data. For categorical analysis, the samples were grouped based on the following age categories: neonatal (0–27 days), infancy (28–364 days), early childhood (1 to <6 years), middle childhood (6 to <12 years), adolescence (12–18 years), and adulthood (>18 years).

Statistical analyses were performed using GraphPad Prism 5 (La Jolla, CA) and Microsoft Excel (365 ProPlus; Redmond, WA). Nonparametric tests were used to test age, sex, and genotype dependence. To compare two groups (e.g., male vs. female), the Mann-Whitney test was used. The Kruskal-Wallis test followed by Dunn's multiple comparison tests were used to perform the age-dependent data analyses and determine associations between the genotype and mRNA expression, protein abundance, and enzyme activity. For correlation analysis, the nonparametric Spearman regression test was used. Additionally, the Jonckheere-Terpstra test and multivariate analysis were performed by using RStudio (version 1.0.136, R version 3.3.2, Boston, MA).

A nonlinear regression equation (eq. 1) was used to fit the ontogeny data, as described previously (Bhatt et al., 2017), where $Adult_{max}$ is the maximum average relative protein abundance, Age is the age in years of the subject at the time of sample collection, Age_{50} is the age in years at which half-maximum adult protein abundance is obtained, E is protein abundance at any given age, E_{birth} is protein abundance at birth, and n is the exponential factor.

$$E = \left(\frac{Adult_{max} - E_{birth}}{Age_{50}^{n} + Age^{n}}\right) \times Age^{n} + E_{birth} \quad (1)$$

For haplotype analysis, the number of variants was directly counted. Hardy-Weinberg equilibrium (HWE) was determined by comparing the variant frequencies with the expected values using a contingency table χ^2 statistic with Yates' correction. The numbers of haplotype and statistics D, D', and LD were estimated by Haploview 4.2 software. Relationships were considered significant at $P < 0.05$.

Results

Hierarchical Clustering of Major Hepatic Drug-Metabolizing Enzymes and Correlation Analysis of UGT2B17 Protein, mRNA, and Activity. Hierarchical clustering analysis of quantitative proteomics results of major hepatic drug-metabolizing enzymes from a preliminary study conducted in first 165 samples (out of a total 455 samples) suggested unique and highly variable protein abundance for UGT2B17 (Supplemental Fig. S1). The correlation between *UGT2B17* mRNA and protein abundance or activity was moderate (r^2 = 0.17 and 0.19, respectively) but statistically significant ($P < 0.0001$) (Supplemental Fig. S2A). Consistent with the literature (Ohtsuki et al., 2012), the correlation between mRNA and protein expression in tissues was weak; in contrast, a strong correlation between protein abundance and activity was observed (Supplemental Fig. S2, B and C). Although our quantitative proteomics method was very sensitive for UGT2B17 detection [lower limit of quantification (LLOQ) = 0.17 pmol/mg of microsomal protein], the protein was not detected in 48% of the samples, indicating a rather large range of variability in protein expression. For statistical analysis, samples below the limit of detection (<LOD) were assigned a value of 0.06 pmol/mg of microsomal protein (i.e., one third of LLOQ) instead of zero. In low UGT2B17 expressers, rates of testosterone- and DHT-glucuronide formation were also consistently low. The average human liver UGT2B17 protein abundance in liver microsomal samples (n = 370, excluding zero copy number samples) was 0.92 ± 1.6 pmol/mg microsomal protein with 162-fold interindividual variability (0.06–9.7 pmol/mg microsomal protein). Mean rates of testosterone- and DHT-glucuronide formation (range; fold difference) were 15.4 (0.3–184; 558) and 41.8 (1.0–233; 233) pmol/min per milligram microsomal protein, respectively (Table 1).

Association of UGT2B17 Protein Abundance, Testosterone/DHT Glucuronide Formation, and Genetic Variation. UGT2B17 protein was detected in 38% and 52% of the samples carrying one and two gene copies, respectively. UGT2B17 protein was undetectable in samples homozygous for the *UGT2B17* gene deletion (CNV = 0). This variability was also reflected by mRNA data demonstrating that FPKM values were significantly higher ($P < 0.0001$) in samples with one or two *UGT2B17* gene copies; however, FPKM values did not differ among the samples with one and two gene copies owing to the high variability (>205-fold) within each group. Samples carrying two *UGT2B17* gene copies showed a 1.7-fold higher mean UGT2B17 protein abundance compared with single gene copy samples (Fig. 1; Table 1). The *UGT2B17* gene-dose-dependent effects on rates of testosterone- and DHT-glucuronide formation rates were consistent with the abundance data (Fig. 1; Table 1). Of the 11 *UGT2B17* SNPs detected in our samples, only four variants (rs7436962, rs9996186, rs28374627, and rs7668258) were associated with mRNA expression, protein abundance, and activity (Supplemental Table S2). Haplotype analyses suggested significant LD between three intronic SNPs (rs7436962, rs9996186, and rs4860305) and a missense SNP rs28374627 (Fig. 1). We identified four haplotypes (H1–H4; Fig. 1) representing combinations of these SNPs with frequency >10% in our sample set. When the diplotypes were compared, samples harboring H3/H4 and H2/H2 haplotypes showed higher UGT2B17 mRNA expression levels, protein abundance, and activity compared with the reference H1/H1 diplotype (Fig. 1; Table 1). The gene-dose effect was also verified by using multivariate analysis (Table 2) and Jonckheere-Terpstra test (Supplemental Table S5)

Association of UGT2B17 Abundance and Testosterone/DHT Glucuronide Formation with Age and Sex. UGT2B17 protein abundance was significantly higher in adulthood compared with infancy and early or middle childhood (Fig. 2A; Supplemental Fig. S3; P values are marked in the figures). Noticeably, the age at which protein expression reaches 50% of that observed in adults (Age_{50}) was >10 years in both male and female samples (Supplemental Fig. S3). Trend analysis (Jonckheere-Terpstra test) showed that there was a statistically significant higher median UGT2B17 abundance with increasing age category (neonatal-infant-early childhood-middle childhood-adolescence- adulthood) (Supplemental Table S5). Male liver donors have a 2.8-fold higher mean UGT2B17 protein level ($P <$ 0.0001) compared with females in samples from donors ≥12 years of age (Fig. 2D; Table 1). Consistent with the protein abundance data, rates of testosterone- and DHT-glucuronide formation were significantly higher in adulthood compared with neonatal, infancy, early childhood, and middle childhood age groups (Fig. 2, E and I). Age-dependent increase in UGT2B17 abundance and activity was greater in male versus female livers (Fig. 2, B, F, and J vs. Fig. 2, C, G, and K). Overall, male liver showed 2- and 1.4-fold higher rates of testosterone- and DHT-glucuronide formation compared with females in samples ≥12 years of age (Fig. 2, H and L).

TABLE 1

Effect of genetic variations, age, and gender on UGT2B17 protein abundance and activity

	Protein Abundance (pmol/mg of Microsomal Protein)					Glucuronide Formation Activity (pmol/min per mg of Microsomal Protein)							
						T-Glucuronide				DHT-Glucuronide			
	n	Mean	Median	Range (Min–Max, Fold Difference)	No. of <LOD Samples	*n*	Mean	Median	Range (Min-Max, Fold Difference)	*n*	Mean	Median	Range (Min–Max, Fold Difference)
All samples[a]	370	0.92	0.06	0.06–9.7, 162	202	325	15.4	6.4	0.3–184, 558	325	41.8	26.2	1.0–233, 233
CN = 0	53	0	0	—	—	46	5.8	3.7	0.6–20.5, 34	46	27.8	21.2	2.6–90.2, 35
CN = 1	172	0.67	0.06	0.06–6.5, 108	107	133	13.8	6.2	0.3–73.6, 223	133	40.8	27.4	1.0–165, 165
CN = 2	198	1.14	0.19	0.06–9.7, 162	95	146	19.9	7.8	0.5–184, 368	146	47	29.5	1.5–233, 155
Diplotypes													
Reference CAGA/CAGA	131	0.57	0.06	0.06–7.9, 132	94	91	13.8	5.7	0.5–123, 246	91	38.7	25.3	2.1–181.4, 86.4
Heterozygous TCAA/CAGG	62	1.59	1.04	0.06–6.02, 100	15	35	27.5	21.4	0.5–98.2, 196	35	63.4	58.8	1.5–160, 107
Homozygous TCAG/TCAG	58	1.63	1.03	0.06–9.7, 162	11	31	30.3	23.2	1.9–184, 96.8	31	66	57	8.3–233, 28
Age categories													
Neonatal	3	0.06	0.06	0.06–0.06	3	3	1.1	0.94	0.4–2.0, 5	3	4.8	3.8	1.6–9.0, 5.6
Infancy	23	0.11	0.06	0.06–0.86, 14.3	20	19	3.3	1.3	0.4–11.5, 29	19	14.1	6.2	1.0–55.1, 55.1
Early childhood	38	0.13	0.06	0.06–1.19, 21	34	29	6.6	3.7	0.3–33.1, 110	29	24.8	17.0	1.0–101, 101
Middle childhood	44	0.15	0.06	0.06–1.49, 24.8	34	35	6.0	3.7	0.7–38.9, 56	35	25.0	16.9	2.6–116, 44.6
Adolescence	61	0.81	0.06	0.06–6.9, 115	33	54	18.8	7.9	0.5–131.3, 263	54	48.5	32.1	2.1–194, 92
Adulthood	185	1.33	0.46	0.06–9.7, 162	76	127	23.2	12.6	0.8–185.8, 232	127	56.3	47.4	3.0–235, 78.3
Gender (age 12 yr)													
Male	149	1.60	0.91	0.06–9.7, 162	60	108	26.9	18.1	0.5–184, 368	108	60.3	47.6	2.1–232, 110
Female	96	0.57	0.06	0.06–5.5, 92	49	73	13.9	9.2	0.79–98, 124	73	43.3	36.2	2.9–160, 55

[a]The samples with zero copy number were excluded from the analysis in all categories except the second row. Thirty-two samples (of 455) were excluded from these analyses because copy number (CN) variation data were not available on these samples.

Association of UGT2B15 Abundance and Testosterone/DHT-Glucuronide Formation with *UGT2B15*2* in Poor UGT2B17 Expressers. An association of the rates of testosterone- or DHT-glucuronide formation with UGT2B15 protein abundance was observed only in samples with low UGT2B17 levels (i.e., <LOD) (Supplemental Fig. S4). Importantly, in these low UGT2B17 expressers, rs1902023, a nonsynonymous *UGT2B15* SNP (Court et al., 2004), was not associated with UGT2B15 protein abundance; however, a significant gene-dose dependent association was found between this SNP and the rates of testosterone- and DHT-glucuronide formation (Fig. 3), respectively. These data suggest that this nonsynonymous UGT2B15 genotype likely affects substrate affinity (k_m) or catalytic activity (k_{cat}) due to a change in amino acid residue in the active or cofactor binding site. Furthermore, the correlation between protein level and activity improved in samples that did not carry heterozygous or homozygous variants of rs1902023 (Supplemental Fig. S4).

Multivariate Linear Regression Analyses. The results were further verified using multivariate linear regression analyses to evaluate associations with UGT2B17 protein abundance and rates of testosterone- or DHT-glucuronide formation as the outcomes and CNV, diplotype, age category, and sex as the predictors. Baseline parameters were set as females, children, reference diplotype (H1/H1), and a copy number of 1 (0 copy number samples were excluded from the analyses). The results of the multivariate linear regression analyses, with missing values imputed, are presented in Table 2. For UGT protein abundance, the coefficient of determination (R^2 value) for the multivariate linear regression was 0.26, indicating that 26% of the variability in UGT2B17 abundance is explained by the predictors in the model. Sex, age categories, and diplotypes were significant predictors of UGT2B17 protein abundance. For testosterone- and DHT-glucuronide formation, the R^2 values for the multivariate linear regression were 0.21 and 0.24, indicating that 21% and 24% of the variability in testosterone- and DHT-glucuronide formation is explained by the predictors in the model, respectively. All other multivariate analysis output parameters are presented in Table 2.

Discussion

Distinct from other major drug-metabolizing enzymes, unusually high interindividual variability was observed for UGT2B17 in our large cohort of human liver tissue samples. The major factors impacting the observed variability include CNVs, SNPs, age, and sex. Developmental *UGT2B17* gene expression and association of SNPs located in the *UGT2B17* gene with its mRNA expression have been previously reported (Burgess et al., 2015; Neumann et al., 2016). Similarly, highly variable protein abundance of UGTs in adult liver is known (Fallon et al., 2013); however, our data are novel in respect to measuring protein abundance by selective LC-MS/MS proteomics, enzyme activity using two probe substrates (testosterone and DHT), and comprehensive CNV and diplotype analyses in the same set of samples. The large cohort of samples allowed comprehensive multivariate analyses, which revealed the individual contributions of many factors impacting UGT2B17 protein abundance and androgen glucuronidation activities. These protein abundance and activity data are important to predict variability in the metabolism of UGT2B17 xenobiotic substrates and sex steroids.

With respect to drug metabolism, UGT2B17 is a less studied enzyme, and no regulatory guidance for industry currently exists for this enzyme. The US Food and Drug Administration and European Medicines Agency recommend in vitro testing for the likelihood of a new chemical entity to be a substrate or inhibitor of other UGT isoforms, such as UGT1A1, UGT1A3, UGT1A4, UGT1A6, UGT1A9, UGT2B7 and UGT2B15. Our data predict that overlooking UGT2B17 could lead to clinical failure of a UGT2B17 substrate drug owing to high PK variability. Indeed, the UGT2B17 substrate MK-7246 was discontinued from clinical trials for high PK variability (Wang et al., 2012). Consistent with the literature (Gallagher et al., 2010), females have lower UGT2B17 expression levels compared with males. Likewise, the distinct ontogeny of UGT2B17 compared with the common drug-metabolizing enzymes, P450s, and other UGTs is an important finding of this study. These data predict that the use of UGT2B17 substrate drugs

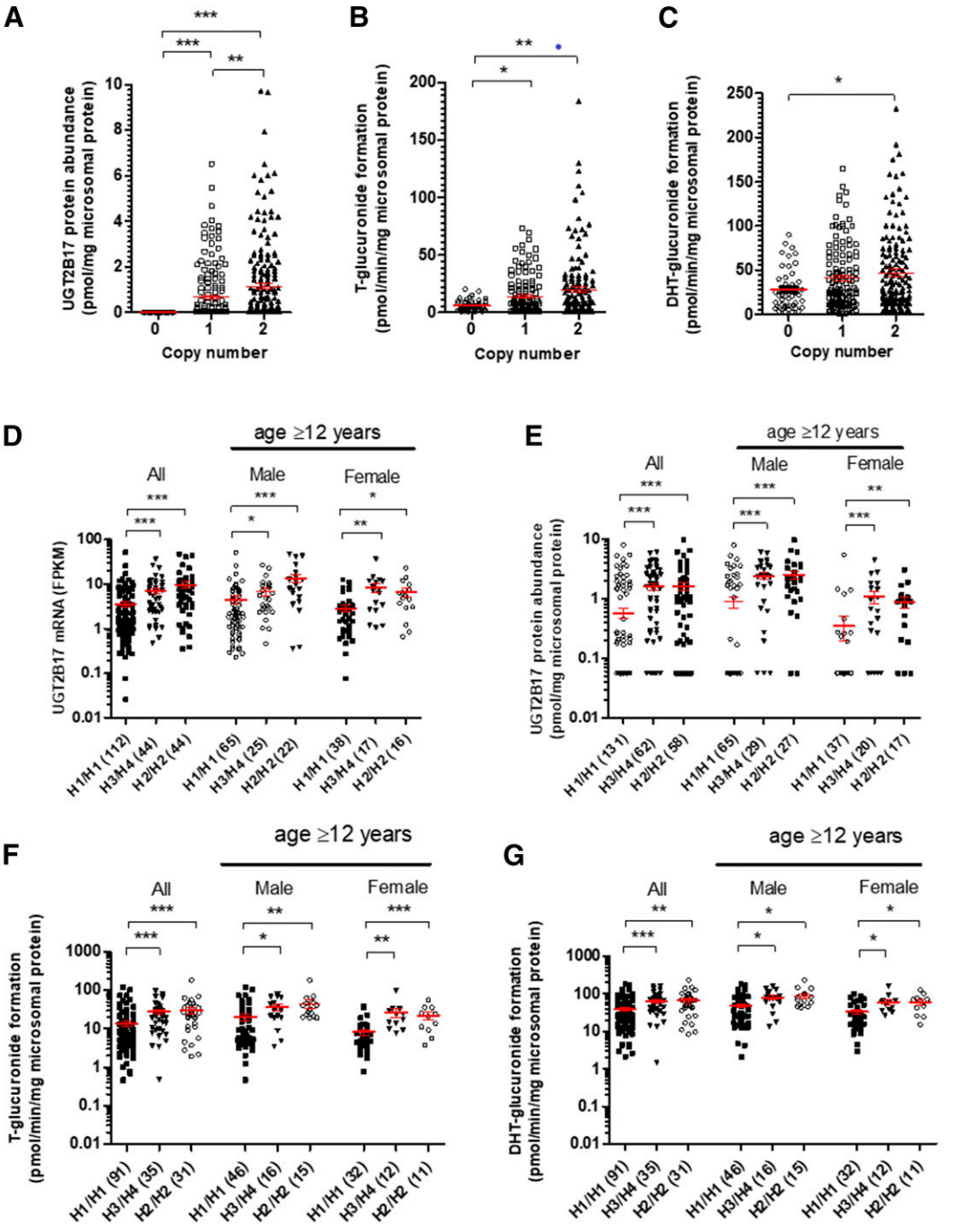

Diplotypes	Haplotypes	UGT2B17 Haplotype Analysis				Frequency
		rs7436962 (Intron) C>T	rs9996186 (Intron) A>C	rs28374627 Synonymous (TYR) G>A	rs4860305 (Intron)A>G	
H1/H1	H1 (homozygous reference)	C	A	G	A	0.50
H2/H2	H2 (homozygous variant)	T	C	A	G	0.22
H3/H4	H3 (heterozygous variant)	T	C	A	A	0.13
	H4 (heterozygous variant)	C	A	G	G	0.12
-	H5	T	C	G	A	0.02

Fig. 1. The *UGT2B17* gene deletion is associated with its protein abundance (A), rates of testosterone- and DHT-glucuronide formation (B and C, respectively). *UGT2B17* diplotypes (haplotype pairs on homologous chromosomes) are associated with UGT2B17 mRNA expression (D), protein abundance (E), testosterone-glucuronide formation (F), and DHT-glucuronide formation (G). Confounding factor, that is, samples from subjects aged younger than 12 years, were excluded from the subanalysis. $^{*}P < 0.05$; $^{**}P < 0.01$; $^{***}P < 0.0001$. Sample number in each group is shown in parentheses in the *x*-axis.

TABLE 2

Multivariate linear regression analysis of predictors associated with interindividual variability of UGT2B17 protein abundance and UGT2B17-mediated testosterone and DHT-glucuronide formation

Dependent Variable	Independent Variable	Effect Size β (Coefficient)	S.E.	*t*-Stat	*P* Value
Protein abundance (pmol/mg of microsomal protein)	Intercept	−1.0	0.28	−3.5	5.8×10^{-4}
	Male	0.84	0.18	4.5	9.7×10^{-6}
	Adolescence	0.48	0.38	1.3	0.21
	Adulthood	1.67	0.25	4.7	4.2×10^{-6}
	Diplotype H3/H4	0.95	0.25	3.8	1.8×10^{-4}
	Diplotype H2/H2	1.1	0.23	4.7	4.2×10^{-6}
	Copy no.: 2	0.22	0.22	1.1	0.31
Testosterone -glucuronide formation (pmol/min per mg of microsomal protein)	Intercept	−13.9	7.0	−2.0	<0.05
	Male	11.7	4.0	2.9	0.004
	Adolescence	15.2	8.8	1.7	0.09
	Adulthood	21.0	6.2	3.4	9.8×10^{-4}
	Diplotype H3/H4	12.7	5.5	2.3	0.02
	Diplotype H2/H2	20.1	5.3	3.8	2.2×10^{-4}
	Copy no.: 2	5.5	4.8	1.1	0.25
DHT-glucuronide formation (pmol/min per mg of microsomal protein)	Intercept	−8.5	11	−0.8	0.44
	Male	15.6	6.4	2.45	0.015
	Adolescence	27.5	14	2.0	<0.05
	Adulthood	42.8	9.9	4.3	2.7×10^{-5}
	Diplotype H3/H4	26.5	8.7	3.1	0.003
	Diplotype H2/H2	31.5	8.4	3.8	0.0002
	Copy no.: 2	2.8	7.6	0.4	0.71

(e.g., vorinostat and lorcaserin) in women and children younger than 12 years could lead to supratherapeutic drug levels. We therefore recommend that UGT2B17 should be included in the in vitro UGT screening panel during early drug discovery, and caution should be taken when designing clinical studies of UGT2B17 substrate drugs in females and children along with consideration of genetic polymorphisms. UGT2B17 is expressed in other organs, such as intestine, appendix, bone marrow, and prostate; however, liver is considered an effective elimination organ for UGT2B17 substrates because of its larger size (resulting high total abundance) and high blood flow. The liver microsomes used in this study were isolated in two different laboratories, and other factors, such as medication use and storage conditions, could affect protein abundance in the microsomes; however, the lack of correlation between UGT2B17 and other proteins (e.g., UGT2B15, Supplemental Fig. S1) in the same samples indicates that the observed UGT2B17 data primarily reflect biologic or interindividual variability.

By regulating testosterone metabolism, UGT2B17 is linked to multiple pathophysiological conditions, such as obesity (Zhu et al., 2015) and prostate cancer (Barbier and Belanger, 2008; Paquet et al., 2012; Kpoghomou et al., 2013; Gauthier-Landry et al., 2015). For example, the *UGT2B17* gene deletion (homozygous) is associated with decreases in fat mass ($P < 0.01$) and insulin sensitivity ($P < 0.05$) (Swanson et al., 2007), and the males with lower testosterone levels are 2.4 times more likely to be obese than males with higher testosterone levels (Mulligan et al., 2006). On the other hand, high UGT2B17 protein levels have been identified as the strongest independent molecular prognostic marker of overall survival in mutated chronic lymphocytic leukemia patients (Bhoi et al., 2016). The *UGT2B17* deletion (homozygous) genotype is associated with a decreased risk of colorectal cancer in men, but it was nonpredictive in women (Angstadt et al., 2013). It is also noteworthy that association studies on UGT2B17 gene deletion and disease risks (e.g., prostate cancer) are controversial. These contradictions in literature could be explained as the published association studies do not acknowledge the effect of confounding factors other than gene deletion (e.g., SNPs and nongenetic factors) on UGT2B17 variability. Further, UGT2B15, which affects testosterone glucuronidation in UGT2B17 poor expressers, has not been considered in these association studies. Therefore, the data presented here will help in designing better clinical studies to investigate association of individual factors affecting UGT2B17 with disease risk.

Although testosterone and its glucuronides are believed to be transported by organic anion polypeptide transporters (OATPs) and multidrug resistance-associated protein (MRPs) (Hamada et al., 2008), the UGT2B17 interindividual variability is significantly greater compared with the variability in transporter abundance previously reported by us in a subset of these samples (Prasad et al., 2014, 2016). Nevertheless, genetic polymorphism in transporters should also be considered when designing clinical studies to investigate association of UGT2B17 variability with testosterone-related clinical outcomes.

UGT2B17 interindividual variability data could also be used to develop a better doping test approach to avoid false-negative or -positive test results. The urinary testosterone (T) to epitestosterone (E) ratio (T/E) has a cutoff limit of 4 and is used to detect T doping in all cases. T is metabolized by UGT2B17, and E is metabolized by UGT2B7. Individuals homozygous for the *UGT2B17* deletion allele excrete negligible amounts of T in urine compared with subjects with one or two gene copies (Bao et al., 2008) and rarely reach the T/E cutoff value of 4 after T doping, indicating that genetic testing for the *UGT2B17* deletion allele may increase the chances of identifying atypical findings, especially in dissecting false-negative test results. Moreover, based on our study, there should be different cutoff values for males versus females, adolescents versus adults, and different haplotypes.

The sex- or age-dependent expression of UGT2B17 may be explained by its regulation by androgens and estradiol. For example, Bao et al. demonstrated that *UGT2B15* and *2B17* are androgen-regulated genes and that androgen receptor (AR) is required for both their basal and androgen-regulated expression (Bao et al., 2008). Similarly, UGT2B17 is 5-fold more abundant in metastatic versus benign prostate cancer samples (Paquet et al., 2012). *UGT2B17* and myeloid cell leukemia-1 (Mcl-1) expression is upregulated in endometrial cancer (EC) tissues, and UGT2B17 depletion induces inhibition of cell growth and apoptosis in EC cells through Mcl-1 downregulation (Hirata et al., 2010); however, UGT2B17 variability within a single group (e.g., adult males)

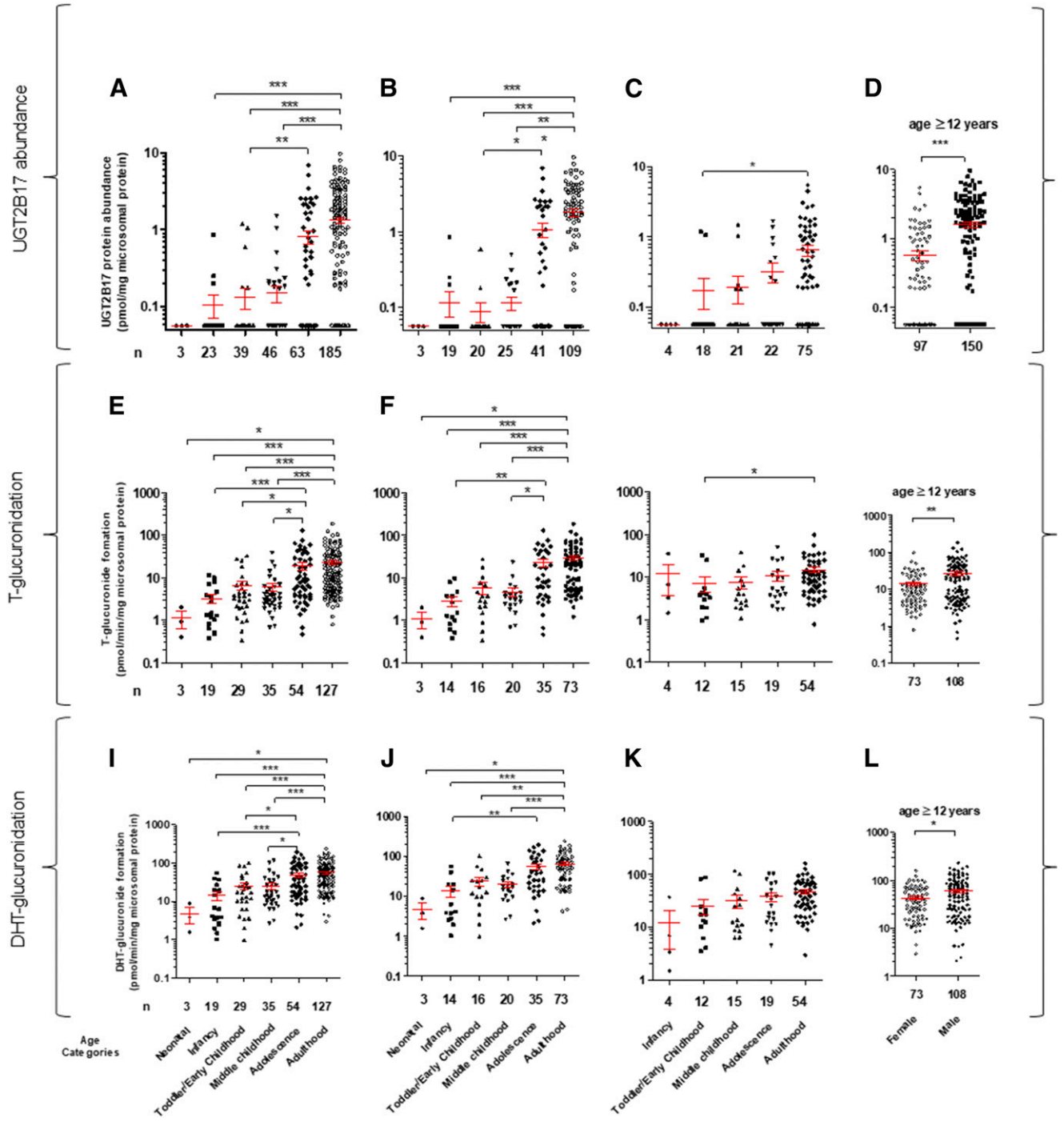

Fig. 2. Categorical age-dependent UGT2B17 protein abundance (A–D), testosterone (T)-glucuronide formation (E–H), and DHT-glucuronide formation (I–L) data in all (A, E, and I), male (B, F and J) and female (C, G, and K) livers. The *x*-axis labels identifying data categories in the bottom panel (I–L) are also applicable to the corresponding top two panels (A–H). Number of samples is presented either as main label in the *x*-axis (A–H) or the *x*-axis parentheses (I–L). Donors with zero *UGT2B17* gene copy were excluded from this analysis. Of 375 samples (male plus female), 205 were lower than the LOD of UGT2B17 protein measurement. For statistical analysis, samples <LOD (excluding zero copy number) were assigned a value of 0.06 pmol/mg of microsomal protein, which was one-third the LLOQ (0.17 pmol/mg of microsomal protein). UGT2B17 was sparsely (12 of 92 samples) detected in children younger than the age of 9 years. An association of age with UGT2B17 abundance or testosterone and DHT-glucuronide formation was more prominent in male versus. female. Mean UGT2B17 protein abundance and testosterone- and DHT-glucuronide formation in these samples was 2.8-, 1.9-, and 1.4-fold greater in male versus female donors aged ≥12 years, respectively (D). $^{*}P < 0.05$; $^{**}P < 0.01$; $^{***}P < 0.0001$.

indicates the involvement of multiple other epigenetic and transcriptional mechanisms. For example, UGT2B15 and UGT2B17 are both negatively regulated by the miR-376c microRNA that binds to the 3′-UTRs of UGT2B15 and UGT2B17 mRNA in prostate cancer cells (Wijayakumara et al., 2015). It has also been shown that Forkhead Box Protein A1 (FOXA1) regulates UGT2B17 gene transcription in LNCaP prostate cancer cells (Hu et al., 2010). Similarly, polymorphic PXR and CAR are associated with altered expression of UGT2Bs, respectively (Verreault et al., 2010). Therefore, SNPs in these polymorphic transcriptional factors [e.g., -298G/G and 11193C/C in

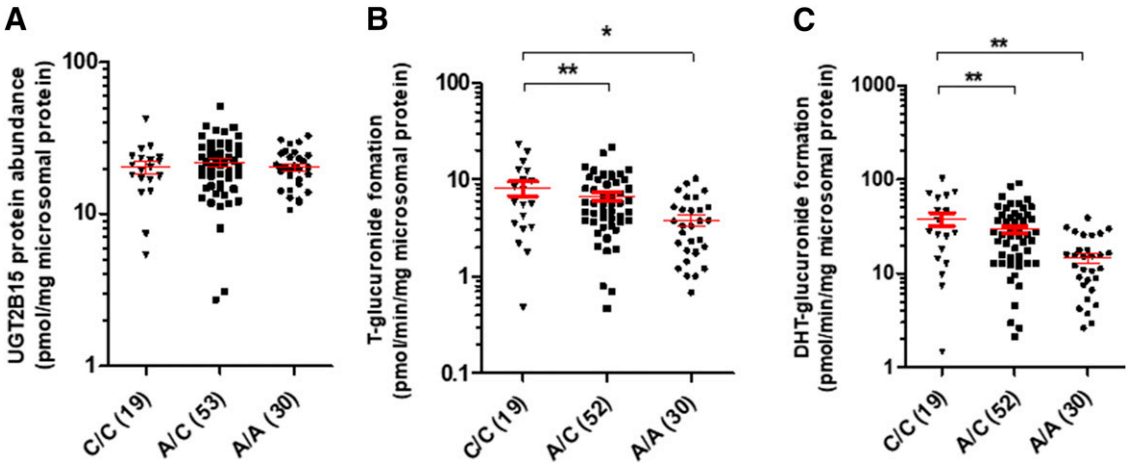

Fig. 3. The *UGT2B15* SNP (rs1902023) is not associated with UGT2B15 protein abundance in low UGT2B17 expressers (A), but it is significantly associated with increased rates of testosterone-glucuronide (B) and DHT-glucuronide (C) formation (picomoles per milligram per minute microsomal protein). Only samples with UGT2B17 abundance <LOD (0.06 pmol/mg of microsomal protein) samples were included in this analysis.

PXR (Du et al., 2013) and IVS2-99C>T in CAR (Urano et al., 2009)] can also indirectly influence UGT2B17 expression. Clearly, further research characterizing the underlying mechanisms contributing to interindividual variability in UGT2B17 abundance and activity is warranted.

Despite the significant physiologic role of testosterone, testosterone replacement therapy (TRT) is controversial. For example, a meta-analysis suggested an association of TRT with prostate cancer; however, many independent studies failed to reproduce this finding (Barbier and Belanger, 2008; Paquet et al., 2012; Kpoghomou et al., 2013; Gauthier-Landry et al., 2015). The Food and Drug Administration recently reissued a black-box warning on TRT because of its association with cardiovascular side effects. UGT2B17 variability should be considered during TRT to ensure safe and effective testosterone use. A similar strategy may also be considered to improve high-testosterone therapy (also referred to as bipolar androgen therapy) in prostate cancer patients (Schweizer et al., 2015).

Taken together, the findings of this study are of clinical importance and can be directly translated to individualize drug therapy of UGT2B17 substrates by stratifying patients based on *UGT2B17* genotype and predicted phenotype. Moreover, physiologically based PK models can be developed based on these data to predict more accurately the UGT2B17-mediated glucuronidation of endobiotics and xenobiotics and translate such data to predicting in vivo disposition of these substrates.

Acknowledgments

We thank Prachi Choudhari and Mikael Boberg for assistance with LC-MS/MS sample analysis; Dr. Kenneth Thummel and Dr. Allan Rettie, UW School of Pharmacy for their valuable suggestions throughout this project; and Amy Turner, Praful Aggarwal, and Rachel Lorier from Dr. Ulrich Broeckel's laboratory to generate a part of the genotyping data.

Authorship Contributions

Participated in research design: Bhatt, Gaedigk, Leeder, Prasad.

Conducted experiments: Bhatt, Basit, Zhang, Claw, Lee, Mehrotra, Prasad, Gaedigk, Pearce, Gaedigk, Broeckel.

Contributed new reagents or analytic tools: Chaudhry, Schuetz, Leeder, Prasad.

Performed data analysis: Bhatt, Basit, Zhang, Claw, Lee, Mehrotra, Gaedigk, Broeckel, Thornton, Prasad, Nickerson.

Wrote or contributed to the writing of the manuscript: Bhatt, Basit, Zhang, Claw, Mehrotra, Gaedigk, Lee, Pearce, Gaedigk, Broeckel, Nickerson, Thornton, Amory, Leeder, Prasad.

References

Angstadt AY, Berg A, Zhu J, Miller P, Hartman TJ, Lesko SM, Muscat JE, Lazarus P, and Gallagher CJ (2013) The effect of copy number variation in the phase II detoxification genes UGT2B17 and UGT2B28 on colorectal cancer risk. *Cancer* **119**:2477–2485.

Bao BY, Chuang BF, Wang Q, Sartor O, Balk SP, Brown M, Kantoff PW, and Lee GSM (2008) Androgen receptor mediates the expression of UDP-glucuronosyltransferase 2 B15 and B17 genes. *Prostate* **68**:839–848.

Barbier O and Bélanger A (2008) Inactivation of androgens by UDP-glucuronosyltransferases in the human prostate. *Best Pract Res Clin Endocrinol Metab* **22**:259–270.

Beaulieu M, Lévesque E, Hum DW, and Bélanger A (1996) Isolation and characterization of a novel cDNA encoding a human UDP-glucuronosyltransferase active on C19 steroids. *J Biol Chem* **271**:22855–22862.

Bhatt DK, Gaedigk A, Pearce RE, Leeder JS, and Prasad B (2017) Age-dependent protein abundance of cytosolic alcohol and aldehyde dehydrogenases in human liver. *Drug Metab Dispos* **45**: 1044–1048.

Bhatt DK and Prasad B (2018) Critical issues and optimized practices in quantification of protein abundance level to determine inter-individual variability in DMET proteins by LC-MS/MS proteomics. *Clin Pharmacol Ther* **103**:619–630.

Bhoi S, Baliakas P, Cortese D, Mattsson M, Engvall M, Smedby KE, Juliusson G, Sutton LA, and Mansouri L (2016) UGT2B17 expression: a novel prognostic marker within IGHV-mutated chronic lymphocytic leukemia? *Haematologica* **101**:e63–e65.

Burgess KS, Philips S, Benson EA, Desta Z, Gaedigk A, Gaedigk R, Segar MW, Liu Y, and Skaar TC (2015) Age-related changes in microRNA expression and pharmacogenes in human liver. *Clin Pharmacol Ther* **98**:205–215.

Chen G, Luo S, Kozlovich S, and Lazarus P (2016a) Association between glucuronidation genotypes and urinary NNAL metabolic phenotypes in smokers. *Cancer Epidemiol Biomarkers Prev* **25**:1175–1184.

Chen SM, Atchley DH, Murphy MA, Gurley BJ, and Kamdem LK (2016b) Impact of UGT2B17 gene deletion on the pharmacokinetics of 17-hydroexemestane in healthy volunteers. *J Clin Pharmacol* **56**:875–884.

Court MH, Hao Q, Krishnaswamy S, Bekaii-Saab T, Al-Rohaimi A, von Moltke LL, and Greenblatt DJ (2004) UDP-glucuronosyltransferase (UGT) 2B15 pharmacogenetics: UGT2B15 D85Y genotype and gender are major determinants of oxazepam glucuronidation by human liver. *J Pharmacol Exp Ther* **310**:656–665.

Du QQ, Wang ZJ, He L, Jiang XH, and Wang L (2013) PXR polymorphisms and their impact on pharmacokinetics/pharmacodynamics of repaglinide in healthy Chinese volunteers. *Eur J Clin Pharmacol* **69**:1917–1925.

Ekström L, Johansson M, and Rane A (2013) Tissue distribution and relative gene expression of UDP-glucuronosyltransferases (2B7, 2B15, 2B17) in the human fetus. *Drug Metab Dispos* **41**: 291–295.

Fallon JK, Neubert H, Hyland R, Goosen TC, and Smith PC (2013) Targeted quantitative proteomics for the analysis of 14 UGT1As and -2Bs in human liver using NanoUPLC-MS/MS with selected reaction monitoring. *J Proteome Res* **12**:4402–4413.

Gallagher CJ, Balliet RM, Sun D, Chen G, and Lazarus P (2010) Sex differences in UDP-glucuronosyltransferase 2B17 expression and activity. *Drug Metab Dispos* **38**:2204–2209.

Gauthier-Landry L, Bélanger A, and Barbier O (2015) Multiple roles for UDP-glucuronosyltransferase (UGT)2B15 and UGT2B17 enzymes in androgen metabolism and prostate cancer evolution. *J Steroid Biochem Mol Biol* **145**:187–192.

Gordon AS, Fulton RS, Qin X, Mardis ER, Nickerson DA, and Scherer S (2016) PGRNseq: a targeted capture sequencing panel for pharmacogenetic research and implementation. *Pharmacogenet Genomics* **26**:161–168.

Gruber M, Bellemare J, Hoermann G, Gleiss A, Porpaczy E, Bilban M, Le T, Zehetmayer S, Mannhalter C, Gaiger A, et al. (2013) Overexpression of uridine diphospho glucuronosyltransferase 2B17 in high-risk chronic lymphocytic leukemia. *Blood* **121**:1175–1183.

Guillemette C (2003) Pharmacogenomics of human UDP-glucuronosyltransferase enzymes. *Pharmacogenomics J* **3**:136–158.

Hamada A, Sissung T, Price DK, Danesi R, Chau CH, Sharifi N, Venzon D, Maeda K, Nagao K, Sparreboom A, et al. (2008) Effect of SLCO1B3 haplotype on testosterone transport and clinical outcome in caucasian patients with androgen-independent prostatic cancer. *Clin Cancer Res* **14**: 3312–3318.

Hirata H, Hinoda Y, Zaman MS, Chen Y, Ueno K, Majid S, Tripsas C, Rubin M, Chen LM, and Dahiya R (2010) Function of UDP-glucuronosyltransferase 2B17 (UGT2B17) is involved in endometrial cancer. *Carcinogenesis* **31**:1620–1626.

Hu DG, Gardner-Stephen D, Severi G, Gregory PA, Treloar J, Giles GG, English DR, Hopper JL, Tilley WD, and Mackenzie PI (2010) A novel polymorphism in a forkhead box A1 (FOXA1) binding site of the human UDP glucuronosyltransferase 2B17 gene modulates promoter activity and is associated with altered levels of circulating androstane-3α,17β-diol glucuronide. *Mol Pharmacol* **78**:714–722.

Hu DG, Selth LA, Tarulli GA, Meech R, Wijayakumara D, Chanawong A, Russell R, Caldas C, Robinson JL, Carroll JS, et al. (2016) Androgen and estrogen receptors in breast cancer coregulate human UDP-glucuronosyltransferases 2B15 and 2B17. *Cancer Res* **76**:5881–5893.

Kpoghomou MA, Soatiana JE, Kalembo FW, Bishwajit G, and Sheng W (2013) UGT2B17 polymorphism and risk of prostate cancer: a meta-analysis. *ISRN Oncol* **2013**:465916.

Lazarus P, Zheng Y, Runkle EA, Muscat JE, and Wiener D (2005) Genotype-phenotype correlation between the polymorphic UGT2B17 gene deletion and NNAL glucuronidation activities in human liver microsomes. *Pharmacogenet Genomics* **15**:769–778.

Luo S, Chen G, Truica C, Baird CC, Leitzel K, and Lazarus P (2017) Role of the UGT2B17 deletion in exemestane pharmacogenetics. *Pharmacogenomics J* DOI: 10.1038/tpj.2017.18 [published ahead of print].

Mulligan T, Frick MF, Zuraw QC, Stemhagen A, and McWhirter C (2006) Prevalence of hypogonadism in males aged at least 45 years: the HIM study. *Int J Clin Pract* **60**:762–769.

Neumann E, Mehboob H, Ramírez J, Mirkov S, Zhang M, and Liu W (2016) Age-dependent hepatic UDP-glucuronosyltransferase gene expression and activity in children. *Front Pharmacol* **7**:437.

Oda S, Fukami T, Yokoi T, and Nakajima M (2015) A comprehensive review of UDP-glucuronosyltransferase and esterases for drug development. *Drug Metab Pharmacokinet* **30**:30–51.

Ohtsuki S, Schaefer O, Kawakami H, Inoue T, Liehner S, Saito A, Ishiguro N, Kishimoto W, Ludwig-Schwellinger E, Ebner T, et al. (2012) Simultaneous absolute protein quantification of transporters, cytochromes P450, and UDP-glucuronosyltransferases as a novel approach for the characterization of individual human liver: comparison with mRNA levels and activities. *Drug Metab Dispos* **40**:83–92.

Pâquet S, Fazli L, Grosse L, Verreault M, Têtu B, Rennie PS, Bélanger A, and Barbier O (2012) Differential expression of the androgen-conjugating UGT2B15 and UGT2B17 enzymes in prostate tumor cells during cancer progression. *J Clin Endocrinol Metab* **97**:E428–E432.

Pearce RE, Gaedigk R, Twist GP, Dai H, Riffel AK, Leeder JS, and Gaedigk A (2016) Developmental expression of CYP2B6: a comprehensive analysis of mRNA expression, protein content and bupropion hydroxylase activity and the impact of genetic variation. *Drug Metab Dispos* **44**:948–958.

Prasad B, Evers R, Gupta A, Hop CE, Salphati L, Shukla S, Ambudkar SV, and Unadkat JD (2014) Interindividual variability in hepatic organic anion-transporting polypeptides and P-glycoprotein (ABCB1) protein expression: quantification by liquid chromatography tandem mass spectroscopy and influence of genotype, age, and sex. *Drug Metab Dispos* **42**:78–88.

Prasad B, Gaedigk A, Vrana M, Gaedigk R, Leeder JS, Salphati L, Chu X, Xiao G, Hop C, Evers R, et al. (2016) Ontogeny of hepatic drug transporters as quantified by LC-MS/MS proteomics. *Clin Pharmacol Ther* **100**:362–370.

Sadeque AJ, Usmani KA, Palamar S, Cerny MA, and Chen WG (2012) Identification of human UDP-glucuronosyltransferases involved in N-carbamoyl glucuronidation of lorcaserin. *Drug Metab Dispos* **40**:772–778.

Schulze JJ, Lundmark J, Garle M, Skilving I, Ekström L, and Rane A (2008) Doping test results dependent on genotype of uridine diphospho-glucuronosyl transferase 2B17, the major enzyme for testosterone glucuronidation. *J Clin Endocrinol Metab* **93**:2500–2506.

Schweizer MT, Antonarakis ES, Wang H, Ajiboye AS, Spitz A, Cao H, Luo J, Haffner MC, Yegnasubramanian S, Carducci MA, et al. (2015) Effect of bipolar androgen therapy for asymptomatic men with castration-resistant prostate cancer: results from a pilot clinical study. *Sci Transl Med* **7**:269ra2.

Shirasaka Y, Chaudhry AS, McDonald M, Prasad B, Wong T, Calamia JC, Fohner A, Thornton TA, Isoherranen N, Unadkat JD, et al. (2016) Interindividual variability of CYP2C19-catalyzed drug metabolism due to differences in gene diplotypes and cytochrome P450 oxidoreductase content. *Pharmacogenomics J* **16**:375–387.

Sun D, Chen G, Dellinger RW, Sharma AK, and Lazarus P (2010) Characterization of 17-dihydroexemestane glucuronidation: potential role of the UGT2B17 deletion in exemestane pharmacogenetics. *Pharmacogenet Genomics* **20**:575–585.

Swanson C, Mellström D, Lorentzon M, Vandenput L, Jakobsson J, Rane A, Karlsson M, Ljunggren O, Smith U, Eriksson AL, et al. (2007) The uridine diphosphate glucuronosyltransferase 2B15 D85Y and 2B17 deletion polymorphisms predict the glucuronidation pattern of androgens and fat mass in men. *J Clin Endocrinol Metab* **92**:4878–4882.

Tanner JA, Prasad B, Claw KG, Stapleton P, Chaudhry A, Schuetz EG, Thummel KE, and Tyndale RF (2017) Predictors of variation in CYP2A6 mRNA, protein, and enzyme activity in a human liver bank: influence of genetic and nongenetic factors. *J Pharmacol Exp Ther* **360**:129–139.

Urano T, Usui T, Shiraki M, Ouchi Y, and Inoue S (2009) Association of a single nucleotide polymorphism in the constitutive androstane receptor gene with bone mineral density. *Geriatr Gerontol Int* **9**:235–241.

Verreault M, Kaeding J, Caron P, Trottier J, Grosse L, Houssin E, Pâquet S, Perreault M, and Barbier O (2010) Regulation of endobiotics glucuronidation by ligand-activated transcription factors: physiological function and therapeutic potential. *Drug Metab Rev* **42**:110–122.

Vrana M, Whittington D, Nautiyal V, and Prasad B (2017) Database of optimized proteomic quantitative methods for human drug disposition-related proteins for applications in physiologically based pharmacokinetic modeling. *CPT Pharmacometrics Syst Pharmacol* **6**:267–276.

Wang YH, Trucksis M, McElwee JJ, Wong PH, Maciolek C, Thompson CD, Prueksaritanont T, Garrett GC, Declercq R, Vets E, et al. (2012) UGT2B17 genetic polymorphisms dramatically affect the pharmacokinetics of MK-7246 in healthy subjects in a first-in-human study. *Clin Pharmacol Ther* **92**:96–102.

Wijayakumara DD, Hu DG, Meech R, McKinnon RA, and Mackenzie PI (2015) Regulation of human UGT2B15 and UGT2B17 by miR-376c in prostate cancer cell lines. *J Pharmacol Exp Ther* **354**:417–425.

Wong NS, Seah EZh, Wang LZ, Yeo WL, Yap HL, Chuah B, Lim YW, Ang PC, Tai BC, Lim R, et al. (2011) Impact of UDP-gluconoryltransferase 2B17 genotype on vorinostat metabolism and clinical outcomes in Asian women with breast cancer. *Pharmacogenet Genomics* **21**:760–768.

Yuan LM, Gao ZZ, Sun HY, Qian SN, Xiao YS, Sun LL, and Zeng S (2016) Inter-isoform heterodimerization of human UDP-glucuronosyltransferases (UGTs) 1A1, 1A9, and 2B7 and impacts on glucuronidation activity. *Sci Rep* **6**:34450.

Zhu AZ, Cox LS, Ahluwalia JS, Renner CC, Hatsukami DK, Benowitz NL, and Tyndale RF (2015) Genetic and phenotypic variation in UGT2B17, a testosterone-metabolizing enzyme, is associated with BMI in males. *Pharmacogenet Genomics* **25**:263–269.

Address correspondence to: Dr. Bhagwat Prasad, Department of Pharmaceutics, University of Washington, 1959 NE Pacific Street, Seattle, WA 98195. E-mail: bhagwat@uw.edu

Supplementary Materials

Hepatic Abundance and Activity of Androgen and Drug Metabolizing Enzyme, UGT2B17, are Associated with Genotype, Age, and Sex

Deepak Kumar Bhatt, Abdul Basit, Haeyoung Zhang, Andrea Gaedigk, Seung-been Lee, Katrina G. Claw, Aanchal Mehrotra, Amarjit Singh Chaudhry, Robin E. Pearce, Roger Gaedigk, Ulrich Broeckel, Timothy A. Thornton, Deborah A. Nickerson, Erin G. Schuetz, John K. Amory, J. Steven Leeder, and Bhagwat Prasad

Department of Pharmaceutics, University of Washington, Seattle, WA, USA (D.K.B., A.B., H.Z., K.G.C., A.M., B.P.)

Division of Pediatric Pharmacology and Medical Toxicology, Department of Pediatrics, Children's Mercy Hospitals and Clinics, Kansas City, MO (A.G., R.E.P., R.G., J.S.L.)

Department of Genome Sciences, University of Washington, Seattle, WA (S.L., D.A.N.)

Department of Pharmaceutical Sciences, St. Jude Children's Research Hospital, Memphis, TN (A.S.C., E.G.S.)

Section of Genomic Pediatrics, Department of Pediatrics, and Human and Molecular Genetics Center, Medical College of Wisconsin, Milwaukee, WI (U.B.)

Department of Biostatistics, University of Washington, Seattle, WA (T.A.T.).

Department of Medicine, University of Washington, Seattle, WA (J.K.A.)

Running title: Interindividual variability in hepatic UGT2B17

Corresponding author: Bhagwat Prasad, Ph.D.; Department of Pharmaceutics, University of Washington, 1959 NE Pacific Street, Seattle, WA 98195, Phone: (206) 221-2295, Fax: (206) 543-3204; E-mail: bhagwat@uw.edu

Materials and Methods

UGT2B17 and UGT2B15 Protein Quantification in HLM Samples

Total protein quantification in HLM samples was performed using a BCA assay kit (Pierce™ BCA Protein Assay Kit). HLMs (80 µL, 2 mg/mL total protein) were digested as described previously (Boberg et al., 2017), with minor modifications. Briefly, microsomal protein and 10 µL of HSA (10 mg/mL) and 10 µL of BSA (0.2 mg/mL) were denatured and reduced with 10 µL of 250 mM DTT and 40 µL of ABB buffer (100 mM) at 95°C for 10 min with gentle shaking at 300 rpm. After cooling to room temperature for 10 minutes, the denatured protein was alkylated by adding 20 µL of 500 mM IAA; the reaction was carried out in the dark for 30 minutes. Ice-cold methanol (500 µL), chloroform (100 µL) and water (400 µL) were subsequently added to each sample. After vortex-mixing and centrifugation at 16,000 × g (4°C) for 5 minutes, the upper and lower layers were removed using vacuum suction and the pellets dried at room temperature for 10 minutes. Pellets were then washed with 500 µL ice-cold methanol and subjected to centrifugation at 8000 × g (4°C) for 5 minutes. After the supernatant was removed, pellets were dried at room temperature for 30 minutes and re-suspended in 60 µL ammonium bicarbonate buffer (ABB) buffer (50 mM, pH 7.8). Subsequently, the protein pellets were digested by adding 20 µL of trypsin (protein: trypsin ratio, approximately 80:1) and incubated at 37°C for 16 hours. The reaction was quenched by the addition of 20 µL of peptide internal standard cocktail (prepared in 80% acetonitrile in water containing 0.5% formic acid) and 10 µL 80% acetonitrile in water containing 0.5% formic acid. The samples were mixed

by vortexing, centrifuged at 4000 × g for 5 min and supernatants collected in LC-MS vials.

The surrogate peptides of UGT2B17 (FSVGYTVEK and SVINDPIYK) and UGT2B15 (SVINDPVYK) were quantified in the digested samples using a validated LC-MS/MS method (Vrana et al., 2017). Light peptides served as calibrators and the corresponding heavy peptides containing terminal labeled [$^{13}C_6$ $^{15}N_2$]-lysine residue served as internal standards. The calibration curve standards ranged from 0.47 to 59.5 and 0.92 to 29.5 fmol (on-column) and were generated by serial dilutions of the UGT2B17 and UGT2B15 protein standards in phosphate buffer (50 mM phosphate buffer, 0.25 M sucrose, 10 mM EDTA, pH 7.4), respectively. Quantification was performed using a triple-quadrupole MS instrument (Sciex Triple Quad™ 6500, Concord, ON) in ESI positive ionization mode coupled to an Acquity UPLC, I-class (Waters, Milford, MA). Five µL of each trypsin digested sample was injected onto the column (ACQUITY UPLC HSS T3 1.8 µm, C_{18} 100A; 100 × 2.1 mm, Waters, Milford, MA). Surrogate light and heavy (internal standards) peptides were monitored using instrument parameters provided in Table 3S. The LC-MS/MS data were processed using Analyst 1.6.2 version software (Sciex, Concord, Ontario). The method was validated for linearity, accuracy and precision (Figure S5 and Table S3).

UGT2B17 Sequencing, Genotyping, Haplotype and Copy Number Variation Analysis

Because liver samples were obtained from different sources, two approaches, gene sequencing and genotyping, were used for genetic characterization of the liver tissue samples (Table S2). The University of Washington and St. Jude Liver Bank samples were sequenced using the PGRN-Seq platform, a targeted sequencing approach, as described elsewhere (Gordon et al., 2016) whereas the samples provided by Children's Mercy (CMH) were genotyped on DMET or PharmacoScan arrays (Affymetrix, Santa Clara, CA, USA). Linkage disequilibrium (LD) analysis of *UGT2B17* variants and inferred haplotypes were determined using Haploview 4.2 (Cambridge, MA, USA).

The UGT2B17 gene was partially covered by PGRNseq. The read depth of UGT2B17 for each sample was obtained from their BAM files using DepthOfCoverage (McKenna et al., 2010). Since *UGT2B17* has a highly related paralog, *UGT2B15*, we used only those reads that mapped uniquely to *UGT2B17* with a mapping quality $\geqslant$20. We also filtered out all base positions with an average sample depth $\geqslant$20 to reduce noise. Next, the mean depth of *UGT2B17* was computed for every sample. To account for individual variation in sequencing efficiency, the mean depth of each sample was normalized by their mean read depth of a control gene, VDR, which was also obtained using DepthOfCoverage. Because the samples were sequenced in two separate runs, normalized read depth was standardized by the respective sequencing run to adjust scaling. The normalized and standardized read depth of the samples showed three distinct distributions that corresponded to a gene copy number of 0, 1 and 2. CNV analysis for the pediatric

samples was done by quantitative multiplex PCR (Gaedigk et al., 2012). Regardless of how CNV was determined, all samples heterozygous for a SNP had a gene copy number of 2 verifying the CNV methods employed. Furthermore, frequencies for zero, 1 and 2 copy number samples in computational analysis (0.12, 0.40 and 0.48) and inquantitative multiplex PCR analysis (0.10, 0.37, 0.53) were comparable.

Analysis of Testosterone, testosterone-Glucuronide, DHT, DHT-Glucuronide and Progesterone in UGT2B17 and UGT2B15 Enzyme Activity Assay

Chromatographic separations of testosterone, testosterone-glucuronide, DHT, DHT-glucuronide and progesterone were performed on an ACQUITY UPLC® BEH C_{18} column (2.1 × 50 mm, 1.7 µm). Mobile phases A and B consisted of water with formic acid 0.1% (v/v) and acetonitrile with formic acid 0.1% (v/v), respectively and were run under gradient conditions at a flow rate of 0.25 mL/min (Table S4). LC and MS/MS parameters used to quantify testosterone, testosterone-glucuronide, DHT, DHT-glucuronide and progesterone are provided in Table S4.

The T and DHT glucuronide method is validated for accuracy, precision and linearity. The accuracy of chromatographic peaks was confirmed by using the stable labeled testosterone-glucuronide-d3 and DHT-glucuronide-d3. The quality control (QC) samples (i.e, analyte standards spiked in the sample matrix containing progesterone as internal standard) were analyzed along with the in vitro samples and inter-day and intra-day precision was calculated.

Table S1. Demographic information of the human liver samples used in this study. Samples analyzed for activity, proteomics, mRNA expression and gene sequencing/genotyping are identified (√) in the Table. The total number of samples analyzed for these assays is presented in the title column (parenthesis).

Sample ID[a]	Age (year)	Sex[b]	Ethnicity[c]	Activity (n=333)	Proteomics (n=455)	mRNA expression (n=230)	Gene sequencing (n=296)[d]	Genotyping (128)[d]	Sourc[e]
86	0.2	M	C	√	√			√	CMKC
95	15.0	M	His	√	√			√	CMKC
99	6.0	M	C	√	√			√	CMKC
105	14.8	M	C	√	√			√	CMKC
142	16.2	M	C	√	√			√	CMKC
195	0.3	M	AA	√	√			√	CMKC
260	2.0	M	C	√	√			√	CMKC
271	0.1	M	AA	√	√			√	CMKC
283	0.5	M	AA	√	√			√	CMKC

Sample ID[a]	Age (year)	Sex[b]	Ethnicity[c]	Activity (n=333)	Proteomics (n=455)	mRNA expression (n=230)	Gene sequencing (n=296)[d]	Genotyping (128)[d]	Sourc[e]
322	1.0	M	His	√	√			√	CMKC
326	14.0	F	C	√	√			√	CMKC
346	3.0	M	C	√	√			√	CMKC
356	8.1	M	AA	√	√			√	CMKC
372	3.0	M	C	√	√			√	CMKC
416	18.0	M	C	√	√			√	CMKC
432	0.0	M	C	√	√			√	CMKC
435	0.8	M	C	√	√			√	CMKC
451	4.6	M	C	√	√			√	CMKC
497	12.4	M	C	√	√			√	CMKC
551	2.0	M	C	√	√			√	CMKC

Sample ID[a]	Age (year)	Sex[b]	Ethnicity[c]	Activity (n=333)	Proteomics (n=455)	mRNA expression (n=230)	Gene sequencing (n=296)[d]	Genotyping (128)[d]	Sourc[e]
569	0.4	M	C	√	√			√	CMKC
596	17.0	F	C	√	√			√	CMKC
613	14.0	M	C	√	√			√	CMKC
617	2.0	F	C	√	√			√	CMKC
620	14.3	M	AA	√	√			√	CMKC
671	0.3	M	His	√	√			√	CMKC
675	5.0	M	C	√	√			√	CMKC
677	2.0	M	AA	√	√			√	CMKC
689	5.0	F	C	√	√			√	CMKC
737	7.3	F	AA	√	√			√	CMKC
738	8.9	F	C	√	√			√	CMKC

Sample ID[a]	Age (year)	Sex[b]	Ethnicity[c]	Activity (n=333)	Proteomics (n=455)	mRNA expression (n=230)	Gene sequencing (n=296)[d]	Genotyping (128)[d]	Sourc[e]
754	11.5	F	PI	√	√			√	CMKC
759	0.1	M	C	√	√			√	CMKC
771	2.7	M	AA	√	√			√	CMKC
774	0.7	M	C	√	√			√	CMKC
776	4.0	F	AA	√	√			√	CMKC
780	0.0	M	AA	√	√			√	CMKC
781	15.0	F	C	√	√			√	CMKC
792	4.0	M	NA	√	√			√	CMKC
811	16.0	M	C	√	√			√	CMKC
825	0.9	M	C	√	√			√	CMKC
845	0.1	M	C	√	√			√	CMKC

Sample ID[a]	Age (year)	Sex[b]	Ethnicity[c]	Activity (n=333)	Proteomics (n=455)	mRNA expression (n=230)	Gene sequencing (n=296)[d]	Genotyping (128)[d]	Sourc[e]
852	2.0	M	His	√	√			√	CMKC
866	3.0	F	C	√	√			√	CMKC
872	2.0	M	C	√	√			√	CMKC
885	17.0	M	AA	√	√			√	CMKC
1055	0.3	M	C	√	√			√	CMKC
1144	12.6	F	U	√	√			√	CMKC
1157	0.1	F	C	√	√			√	CMKC
1181	8.2	M	C	√	√			√	CMKC
1256	13.9	M	C	√	√			√	CMKC
1281	0.6	M	AA	√	√			√	CMKC
1284	3.3	F	AA	√	√			√	CMKC

Sample ID[a]	Age (year)	Sex[b]	Ethnicity[c]	Activity (n=333)	Proteomics (n=455)	mRNA expression (n=230)	Gene sequencing (n=296)[d]	Genotyping (128)[d]	Sourc[e]
1296	0.3	M	AA	√	√			√	CMKC
1297	15.2	M	AA	√	√			√	CMKC
1325	0.5	F	AA	√	√			√	CMKC
1409	18.0	M	C	√	√			√	CMKC
1443	0.9	F	AA	√	√			√	CMKC
1547	0.7	M	AA	√	√			√	CMKC
1624	3.2	F	C	√	√			√	CMKC
1670	13.3	M	C	√	√			√	CMKC
1791	2.8	F	AA	√	√			√	CMKC
1860	8.0	M	C	√	√			√	CMKC
1904	0.3	M	AA	√	√			√	CMKC

Sample ID[a]	Age (year)	Sex[b]	Ethnicity[c]	Activity (n=333)	Proteomics (n=455)	mRNA expression (n=230)	Gene sequencing (n=296)[d]	Genotyping (128)[d]	Sourc[e]
1908	14.0	M	C	√	√			√	CMKC
4591	16.6	F	C	√	√			√	CMKC
4638	15.1	F	C	√	√			√	CMKC
4722	14.5	M	C	√	√			√	CMKC
4787	12.9	M	AA	√	√			√	CMKC
4906	16.8	F	C	√	√			√	CMKC
4907	4.8	F	AA	√	√			√	CMKC
4925	13.2	M	AA	√	√			√	CMKC
5077	16.7	F	C	√	√			√	CMKC
5173	10.8	F	C	√	√			√	CMKC
5242	15.3	M	C	√	√			√	CMKC

Sample ID[a]	Age (year)	Sex[b]	Ethnicity[c]	Activity (n=333)	Proteomics (n=455)	mRNA expression (n=230)	Gene sequencing (n=296)[d]	Genotyping (128)[d]	Sourc[e]
8703	10.0	F	U	√	√			√	CMKC
8804	14.0	M	U	√	√			√	CMKC
8901	6.0	F	U	√	√			√	CMKC
8902	7.0	M	U	√	√			√	CMKC
8906	12.0	M	U	√	√			√	CMKC
8909	9.0	F	U	√	√			√	CMKC
8910	14.0	M	U	√	√			√	CMKC
8912	12.0	F	U	√	√			√	CMKC
8917	6.0	F	U	√	√			√	CMKC
8920	11.0	M	U	√	√			√	CMKC
8924	9.0	F	U	√	√			√	CMKC

Sample ID[a]	Age (year)	Sex[b]	Ethnicity[c]	Activity (n=333)	Proteomics (n=455)	mRNA expression (n=230)	Gene sequencing (n=296)[d]	Genotyping (128)[d]	Sourc[e]
8925	8.0	M	U	√	√			√	CMKC
8926	1.8	F	U	√	√			√	CMKC
8935	17.0	M	U	√	√			√	CMKC
9003	7.0	F	U	√	√			√	CMKC
9005	17.0	M	U	√	√			√	CMKC
9006	10.0	M	U	√	√			√	CMKC
9011	3.0	F	U	√	√			√	CMKC
9013	11.0	M	U	√	√			√	CMKC
9022	5.0	U	U	√	√			√	CMKC
9023	2.6	F	U	√	√			√	CMKC
9027	12.0	M	U	√	√			√	CMKC

Sample ID[a]	Age (year)	Sex[b]	Ethnicity[c]	Activity (n=333)	Proteomics (n=455)	mRNA expression (n=230)	Gene sequencing (n=296)[d]	Genotyping (128)[d]	Sourc[e]
9028	8.0	F	U	√	√			√	CMKC
9031	17.0	F	U	√	√			√	CMKC
9032	14.0	M	U	√	√			√	CMKC
9036	5.0	F	U	√	√			√	CMKC
9101	2.0	M	U	√	√			√	CMKC
9105	17.0	M	U	√	√			√	CMKC
9127	15.0	M	U	√	√			√	CMKC
9507	14.0	M	U	√	√			√	CMKC
9608	4.0	M	U	√	√			√	CMKC
9609	4.0	M	U	√	√			√	CMKC
9611	9.0	M	U	√	√			√	CMKC

Sample ID[a]	Age (year)	Sex[b]	Ethnicity[c]	Activity (n=333)	Proteomics (n=455)	mRNA expression (n=230)	Gene sequencing (n=296)[d]	Genotyping (128)[d]	Sourc[e]
9612	3.0	M	U	√	√			√	CMKC
70874	6.0	M	AA	√	√			√	CMKC
70896	7.0	M	C	√	√			√	CMKC
70898	7.0	M	C	√	√			√	CMKC
70915	7.0	F	C	√	√			√	CMKC
70921	6.0	F	C	√	√			√	CMKC
70953	7.0	F	C	√	√			√	CMKC
70958	8.0	U	U	√	√			√	CMKC
70994	16.0	M	C	√	√			√	CMKC
71000	6.0	M	C	√	√			√	CMKC
71002	5.0	M	C	√	√			√	CMKC

Sample ID[a]	Age (year)	Sex[b]	Ethnicity[c]	Activity (n=333)	Proteomics (n=455)	mRNA expression (n=230)	Gene sequencing (n=296)[d]	Genotyping (128)[d]	Sourc[e]
71165	16.0	F	C	√	√			√	CMKC
71281	16.0	M	C	√	√			√	CMKC
71307	12.0	F	C	√	√			√	CMKC
71414	8.0	M	C	√	√			√	CMKC
71649	15.0	F	C	√	√			√	CMKC
85551	8.0	M	AA	√	√			√	CMKC
85651	12.0	F	AA	√	√			√	CMKC
85891	17.0	F	C	√	√			√	CMKC
99377	11.0	M	C	√	√			√	CMKC
HL102	21.0	M	C		√	√	√		UW
HL103	15.0	F	C		√				UW

Sample ID[a]	Age (year)	Sex[b]	Ethnicity[c]	Activity (n=333)	Proteomics (n=455)	mRNA expression (n=230)	Gene sequencing (n=296)[d]	Genotyping (128)[d]	Sourc[e]
HL105	21.0	M	AA		√	√	√		UW
HL106	45.0	F	C		√	√	√		UW
HL108	42.0	F	C		√	√	√		UW
HL111	28.0	M	C		√	√	√		UW
HL112	28.0	M	C		√	√	√		UW
HL113	9.0	F	C		√	√	√		UW
HL114	19.0	M	C		√	√	√		UW
HL115	52.0	F	C		√	√	√		UW
HL118	25.0	M	C	√	√	√	√		UW
HL119	24.0	M	C		√	√	√		UW
HL120	45.0	F	C	√	√	√	√		UW

Sample ID[a]	Age (year)	Sex[b]	Ethnicity[c]	Activity (n=333)	Proteomics (n=455)	mRNA expression (n=230)	Gene sequencing (n=296)[d]	Genotyping (128)[d]	Sourc[e]
HL121	59.0	F	C		√	√	√		UW
HL125	32.0	M	C		√	√	√		UW
HL127	38.0	M	C		√	√	√		UW
HL128	51.0	M	C	√	√	√	√		UW
HL129	36.0	F	C	√	√	√	√		UW
HL131	62.0	F	C	√	√	√	√		UW
HL132	50.0	F	C		√	√	√		UW
HL133	45.0	F	C	√	√	√	√		UW
HL134	7.0	M	C		√	√	√		UW
HL135	45.0	F	C	√	√	√	√		UW
HL136	39.0	M	C		√	√	√		UW

Sample ID[a]	Age (year)	Sex[b]	Ethnicity[c]	Activity (n=333)	Proteomics (n=455)	mRNA expression (n=230)	Gene sequencing (n=296)[d]	Genotyping (128)[d]	Sourc[e]
HL137	11.0	M	AA	√	√	√	√		UW
HL138	9.0	F	C		√	√	√		UW
HL139	15.0	F	C	√	√	√	√		UW
HL141	59.0	M	C	√	√	√	√		UW
HL143	48.0	M	C	√	√	√	√		UW
HL144	68.0	F	C	√	√	√	√		UW
HL145	38.0	M	C	√	√	√	√		UW
HL146	10.0	M	C	√	√	√	√		UW
HL147	70.0	F	C	√	√	√	√		UW
HL148	60.0	F	C	√	√	√	√		UW
HL149	63.0	F	C	√	√	√	√		UW

Sample ID[a]	Age (year)	Sex[b]	Ethnicity[c]	Activity (n=333)	Proteomics (n=455)	mRNA expression (n=230)	Gene sequencing (n=296)[d]	Genotyping (128)[d]	Sourc[e]
HL150	30.0	M	C	√	√	√	√		UW
HL152	64.0	F	C	√	√	√	√		UW
HL153	59	F	C	√	√	√	√		UW
HL154	26.0	M	C	√	√	√	√		UW
HL155	21.0	M	C	√	√	√	√		UW
HL156	44.0	M	C		√	√	√		UW
HL157	41.0	F	C		√	√	√		UW
HL158	59.0	M	C	√	√	√	√		UW
HL159	53.0	F	C	√	√	√	√		UW
HL160	67.0	M	C	√	√	√	√		UW
HL161	53.0	M	C	√	√	√	√		UW

Sample ID[a]	Age (year)	Sex[b]	Ethnicity[c]	Activity (n=333)	Proteomics (n=455)	mRNA expression (n=230)	Gene sequencing (n=296)[d]	Genotyping (128)[d]	Sourc[e]
HL163	55.0	M	C	√	√	√	√		UW
HL164	50.0	F	C		√	√	√		UW
HL165	61.0	M	A	√	√	√	√		UW
HL166	59.0	F	C		√	√	√		UW
HL167	44.0	M	C	√	√	√	√		UW
HL168	43.0	M	C	√	√	√			UW
HL169	57.0	M	C	√	√	√			UW
HL170	50.0	M	C	√	√	√			UW
HL171	47.0	F	C		√	√			UW
HL172	28.0	M	C		√	√			UW
SJLB1002	30.0	M	C		√		√		SJ

Sample ID[a]	Age (year)	Sex[b]	Ethnicity[c]	Activity (n=333)	Proteomics (n=455)	mRNA expression (n=230)	Gene sequencing (n=296)[d]	Genotyping (128)[d]	Sourc[e]
SJLB1009	60.0	M	U		√		√		SJ
SJLB1038	24.0	M	C		√		√		SJ
SJLB1049	27.0	F	C	√	√	√	√		SJ
SJLB1066	U	M	U	√	√	√	√		SJ
SJLB1069	U	M	U	√	√	√	√		SJ
SJLB1093	66.0	F	U	√	√	√	√		SJ
SJLB1103	68.0	M	C	√	√	√	√		SJ
SJLB1106	62.0	M	C	√	√		√		SJ
SJLB1107	36.0	F	C	√	√	√	√		SJ
SJLB1108	43.0	F	C	√	√	√	√		SJ
SJLB1111	U	M	U		√		√		SJ

Sample ID[a]	Age (year)	Sex[b]	Ethnicity[c]	Activity (n=333)	Proteomics (n=455)	mRNA expression (n=230)	Gene sequencing (n=296)[d]	Genotyping (128)[d]	Sourc[e]
SJLB1122	61.0	F	C	√	√	√	√		SJ
SJLB1125	30.0	F	C	√	√		√		SJ
SJLB116	6.0	F	C		√		√		SJ
SJLB117	1.0	F	C	√	√		√		SJ
SJLB12	66.0	F	C	√	√	√	√		SJ
SJLB120	7.0	M	C		√		√		SJ
SJLB1247	62.0	F	C	√	√		√		SJ
SJLB1255	59.0	F	C	√	√	√	√		SJ
SJLB1256	46.0	M	C		√	√	√		SJ
SJLB127	1.0	M	C		√		√		SJ
SJLB1276	46.0	F	C		√	√	√		SJ

Sample ID[a]	Age (year)	Sex[b]	Ethnicity[c]	Activity (n=333)	Proteomics (n=455)	mRNA expression (n=230)	Gene sequencing (n=296)[d]	Genotyping (128)[d]	Sourc[e]
SJLB128	0	F	C	√	√	√	√		SJ
SJLB129	10.0	F	C		√	√	√		SJ
SJLB1330	40.0	M	C	√	√	√	√		SJ
SJLB1361	10.0	F	C	√	√		√		SJ
SJLB1370	46.0	M	C		√	√	√		SJ
SJLB138	26.0	F	C	√	√	√	√		SJ
SJLB1385	19.0	M	C	√	√	√	√		SJ
SJLB1401	50.0	F	C	√	√	√	√		SJ
SJLB1412	U	M	U	√	√	√	√		SJ
SJLB1435	34.0	M	C		√		√		SJ
SJLB1449	U	U	U	√	√	√	√		SJ

Sample ID[a]	Age (year)	Sex[b]	Ethnicity[c]	Activity (n=333)	Proteomics (n=455)	mRNA expression (n=230)	Gene sequencing (n=296)[d]	Genotyping (128)[d]	Sourc[e]
SJLB1452	U	M	U	√	√	√	√		SJ
SJLB1454	U	M	C	√	√	√	√		SJ
SJLB1457	U	M	C		√	√	√		SJ
SJLB1459	U	M	C	√	√	√	√		SJ
SJLB1461	U	F	U		√		√		SJ
SJLB1463	U	U	U	√	√	√	√		SJ
SJLB1464	U	M	U		√	√	√		SJ
SJLB1466	U	F	U	√	√	√	√		SJ
SJLB1468	U	U	U	√	√	√	√		SJ
SJLB1473	U	F	U	√	√		√		SJ
SJLB1482	U	F	U	√	√	√	√		SJ

Sample ID[a]	Age (year)	Sex[b]	Ethnicity[c]	Activity (n=333)	Proteomics (n=455)	mRNA expression (n=230)	Gene sequencing (n=296)[d]	Genotyping (128)[d]	Sourc[e]
SJLB152	40.0	F	C	√	√	√	√		SJ
SJLB156	20.0	M	C	√	√	√	√		SJ
SJLB157	9.0	M	C	√	√	√	√		SJ
SJLB160	57.0	M	C	√	√	√	√		SJ
SJLB172	16.0	M	C	√	√		√		SJ
SJLB174	23.0	F	C	√	√	√	√		SJ
SJLB175	32.0	M	C	√	√	√	√		SJ
SJLB18	2.0	F	C		√	√	√		SJ
SJLB187	71.0	F	C		√		√		SJ
SJLB200	2.0	F	C	√	√	√	√		SJ
SJLB201	6.0	M	C	√	√		√		SJ

Sample ID[a]	Age (year)	Sex[b]	Ethnicity[c]	Activity (n=333)	Proteomics (n=455)	mRNA expression (n=230)	Gene sequencing (n=296)[d]	Genotyping (128)[d]	Sourc[e]
SJLB203	13.0	M	C	√	√		√		SJ
SJLB205	14.0	F	C	√	√		√		SJ
SJLB206	9.0	M	C	√	√		√		SJ
SJLB209	59.0	F	C	√	√	√	√		SJ
SJLB21	1.0	M	C	√	√				SJ
SJLB217	20.0	M	C	√	√		√		SJ
SJLB221	16.0	M	C	√	√				SJ
SJLB223	14.0	M	C	√	√	√	√		SJ
SJLB229	14.0	M	C	√	√		√		SJ
SJLB251	7.0	M	C		√		√		SJ
SJLB255	6.0	M	C	√	√		√		SJ

Sample ID[a]	Age (year)	Sex[b]	Ethnicity[c]	Activity (n=333)	Proteomics (n=455)	mRNA expression (n=230)	Gene sequencing (n=296)[d]	Genotyping (128)[d]	Sourc[e]
SJLB265	23.0	F	C		√	√	√		SJ
SJLB267	31.0	M	C		√		√		SJ
SJLB269	18.0	M	C		√		√		SJ
SJLB273	5.0	M	C		√	√	√		SJ
SJLB274	1.0	M	C	√	√		√		SJ
SJLB275	13.0	M	C		√		√		SJ
SJLB282	17.0	M	C	√	√		√		SJ
SJLB283	6.0	M	C		√				SJ
SJLB286	9.0	M	C		√				SJ
SJLB287	4.0	F	C		√		√		SJ
SJLB296	7.0	F	C		√	√	√		SJ

Sample ID[a]	Age (year)	Sex[b]	Ethnicity[c]	Activity (n=333)	Proteomics (n=455)	mRNA expression (n=230)	Gene sequencing (n=296)[d]	Genotyping (128)[d]	Sourc[e]
SJLB30	1.0	M	C		√	√	√		SJ
SJLB301	13.0	F	C	√	√				SJ
SJLB304	13.0	M	C		√		√		SJ
SJLB305	18.0	M	C		√	√	√		SJ
SJLB306	5.0	M	C		√	√	√		SJ
SJLB307	2.0	M	C		√	√	√		SJ
SJLB310	3.0	F	C		√		√		SJ
SJLB315	2.0	M	C		√	√	√		SJ
SJLB319	30.0	M	C	√	√	√	√		SJ
SJLB320	25.0	M	C		√	√	√		SJ
SJLB323	43.0	M	C		√		√		SJ

Sample ID[a]	Age (year)	Sex[b]	Ethnicity[c]	Activity (n=333)	Proteomics (n=455)	mRNA expression (n=230)	Gene sequencing (n=296)[d]	Genotyping (128)[d]	Sourc[e]
SJLB325	60.0	M	C	√	√	√	√		SJ
SJLB329	32.0	M	C	√	√	√	√		SJ
SJLB331	62.0	F	C	√	√	√	√		SJ
SJLB332	65.0	F	C	√	√		√		SJ
SJLB333	59.0	M	C	√	√	√	√		SJ
SJLB334	63.0	M	C	√	√	√	√		SJ
SJLB335	36.0	M	C	√	√	√	√		SJ
SJLB336	70.0	M	C	√	√	√	√		SJ
SJLB338	59.0	M	C		√		√		SJ
SJLB34	0	M	C		√	√	√		SJ
SJLB340	52.0	M	C	√	√	√	√		SJ

Sample ID[a]	Age (year)	Sex[b]	Ethnicity[c]	Activity (n=333)	Proteomics (n=455)	mRNA expression (n=230)	Gene sequencing (n=296)[d]	Genotyping (128)[d]	Sourc[e]
SJLB341	2.0	M	C		√	√	√		SJ
SJLB342	43.0	M	C	√	√	√	√		SJ
SJLB343	35.0	M	C	√	√		√		SJ
SJLB344	63.0	M	C	√	√				SJ
SJLB346	24.0	M	C	√	√		√		SJ
SJLB347	4.0	F	C	√	√	√	√		SJ
SJLB348	43.0	M	C	√	√		√		SJ
SJLB349	2.0	M	C		√	√	√		SJ
SJLB351	49.0	M	C	√	√	√	√		SJ
SJLB355	40.0	M	C	√	√	√	√		SJ
SJLB358	53.0	M	C	√	√				SJ

Sample ID[a]	Age (year)	Sex[b]	Ethnicity[c]	Activity (n=333)	Proteomics (n=455)	mRNA expression (n=230)	Gene sequencing (n=296)[d]	Genotyping (128)[d]	Sourc[e]
SJLB36	1.0	M	C	√	√	√	√		SJ
SJLB360	54.0	M	C	√	√				SJ
SJLB361	63.0	M	C	√	√	√	√		SJ
SJLB363	46.0	M	C		√		√		SJ
SJLB365	28.0	M	C	√	√	√	√		SJ
SJLB366	60.0	F	C	√	√	√	√		SJ
SJLB369	66.0	F	C	√	√		√		SJ
SJLB370	45.0	M	C	√	√		√		SJ
SJLB372	37.0	M	C	√	√	√	√		SJ
SJLB374	72.0	M	C	√	√		√		SJ
SJLB376	47.0	M	C	√	√	√	√		SJ

Sample ID[a]	Age (year)	Sex[b]	Ethnicity[c]	Activity (n=333)	Proteomics (n=455)	mRNA expression (n=230)	Gene sequencing (n=296)[d]	Genotyping (128)[d]	Sourc[e]
SJLB378	81.0	M	C	√	√	√	√		SJ
SJLB379	34.0	M	C	√	√	√	√		SJ
SJLB38	64.0	F	C		√				SJ
SJLB380	9.0	M	C	√	√	√	√		SJ
SJLB381	14.0	M	C	√	√	√	√		SJ
SJLB383	61.0	M	C	√	√	√	√		SJ
SJLB386	54.0	M	C	√	√		√		SJ
SJLB387	66.0	M	C		√		√		SJ
SJLB389	22.0	M	C	√	√	√	√		SJ
SJLB39	56.0	M	C	√	√		√		SJ
SJLB393	3.0	M	C		√	√	√		SJ

Sample ID[a]	Age (year)	Sex[b]	Ethnicity[c]	Activity (n=333)	Proteomics (n=455)	mRNA expression (n=230)	Gene sequencing (n=296)[d]	Genotyping (128)[d]	Sourc[e]
SJLB401	38.0	F	C	√	√				SJ
SJLB403	73.0	M	C		√	√	√		SJ
SJLB407	44.0	M	C		√	√	√		SJ
SJLB408	32.0	F	C	√	√	√	√		SJ
SJLB409	29.0	M	C	√	√	√	√		SJ
SJLB413	44.0	M	C	√	√	√	√		SJ
SJLB414	29.0	M	C		√	√	√		SJ
SJLB415	2.0	F	C		√	√	√		SJ
SJLB416	11.0	F	C		√		√		SJ
SJLB417	46.0	M	C		√		√		SJ
SJLB418	16.0	F	C	√	√	√	√		SJ

Sample ID[a]	Age (year)	Sex[b]	Ethnicity[c]	Activity (n=333)	Proteomics (n=455)	mRNA expression (n=230)	Gene sequencing (n=296)[d]	Genotyping (128)[d]	Sourc[e]
SJLB419	0	M	C	√	√		√		SJ
SJLB426	43.0	F	C	√	√	√	√		SJ
SJLB437	62.0	F	C	√	√				SJ
SJLB438	7.0	F	C	√	√	√	√		SJ
SJLB439	48.0	M	C	√	√				SJ
SJLB444	12.0	M	C		√		√		SJ
SJLB450C	40.0	M	C		√				SJ
SJLB459	17.0	F	C		√		√		SJ
SJLB465	61.0	F	C	√	√		√		SJ
SJLB467	U	F	U	√	√	√	√		SJ
SJLB469	28.0	M	C	√	√	√	√		SJ

Sample ID[a]	Age (year)	Sex[b]	Ethnicity[c]	Activity (n=333)	Proteomics (n=455)	mRNA expression (n=230)	Gene sequencing (n=296)[d]	Genotyping (128)[d]	Sourc[e]
SJLB475	70.0	F	C	√	√				SJ
SJLB476	66.0	F	C	√	√	√	√		SJ
SJLB478	56.0	F	C		√	√	√		SJ
SJLB485	50.0	F	C	√	√	√	√		SJ
SJLB486	17.0	M	C	√	√		√		SJ
SJLB505	24.0	M	C	√	√	√	√		SJ
SJLB51	68.0	M	C		√				SJ
SJLB550	U	U	C		√	√	√		SJ
SJLB618B	56.0	M	C		√	√	√		SJ
SJLB627B	74.0	F	C		√	√	√		SJ
SJLB629	50.0	F	C		√		√		SJ

Sample ID[a]	Age (year)	Sex[b]	Ethnicity[c]	Activity (n=333)	Proteomics (n=455)	mRNA expression (n=230)	Gene sequencing (n=296)[d]	Genotyping (128)[d]	Sourc[e]
SJLB631	65.0	M	C	√	√	√	√		SJ
SJLB633B	15.0	M	C		√		√		SJ
SJLB636	47.0	M	C		√				SJ
SJLB638	57.0	M	C		√	√	√		SJ
SJLB64	23.0	F	C	√	√		√		SJ
SJLB640	62.0	M	C		√				SJ
SJLB644	60.0	F	C	√	√	√	√		SJ
SJLB651	17.0	F	C	√	√	√	√		SJ
SJLB653B	61.0	M	C		√	√	√		SJ
SJLB662	35.0	F	C	√	√	√	√		SJ
SJLB667B	28.0	F	C		√				SJ

Sample ID[a]	Age (year)	Sex[b]	Ethnicity[c]	Activity (n=333)	Proteomics (n=455)	mRNA expression (n=230)	Gene sequencing (n=296)[d]	Genotyping (128)[d]	Sourc[e]
SJLB669B	66.0	F	C		√	√	√		SJ
SJLB670B	49.0	F	C		√	√	√		SJ
SJLB671	3.0	F	C		√	√	√		SJ
SJLB673B	52.0	M	C		√	√	√		SJ
SJLB675	69.0	F	C	√	√				SJ
SJLB678B	68.0	F	C		√	√	√		SJ
SJLB679B	11.0	M	U		√				SJ
SJLB682B	50.0	F	C		√				SJ
SJLB683B	49.0	F	C		√	√	√		SJ
SJLB684B	54.0	M	C		√	√	√		SJ
SJLB70	48.0	F	C		√		√		SJ

Sample ID[a]	Age (year)	Sex[b]	Ethnicity[c]	Activity (n=333)	Proteomics (n=455)	mRNA expression (n=230)	Gene sequencing (n=296)[d]	Genotyping (128)[d]	Sourc[e]
SJLB704	51.0	M	C	√	√	√	√		SJ
SJLB705	71.0	F	C	√	√	√	√		SJ
SJLB706	66.0	F	C	√	√	√	√		SJ
SJLB707	66.0	F	C	√	√		√		SJ
SJLB709	60.0	M	C	√	√	√	√		SJ
SJLB711	73.0	M	C	√	√	√	√		SJ
SJLB713	20.0	M	C		√	√	√		SJ
SJLB715	58.0	M	C	√	√	√	√		SJ
SJLB719	30.0	M	C	√	√	√	√		SJ
SJLB724	61.0	M	C		√	√	√		SJ
SJLB727	1.0	M	C	√	√	√	√		SJ

Sample ID[a]	Age (year)	Sex[b]	Ethnicity[c]	Activity (n=333)	Proteomics (n=455)	mRNA expression (n=230)	Gene sequencing (n=296)[d]	Genotyping (128)[d]	Sourc[e]
SJLB730	57.0	M	C	√	√	√	√		SJ
SJLB733B	49.0	M	C		√	√	√		SJ
SJLB734	0	F	AA	√	√	√	√		SJ
SJLB740	3.0	F	C	√	√		√		SJ
SJLB75	58.0	F	C		√		√		SJ
SJLB750	50.0	M	C	√	√		√		SJ
SJLB753	16.0	F	C	√	√	√	√		SJ
SJLB758	56.0	M	C	√	√	√	√		SJ
SJLB764	0	M	U	√	√	√	√		SJ
SJLB767	30.0	F	C	√	√	√	√		SJ
SJLB769	35.0	F	C		√		√		SJ

Sample ID[a]	Age (year)	Sex[b]	Ethnicity[c]	Activity (n=333)	Proteomics (n=455)	mRNA expression (n=230)	Gene sequencing (n=296)[d]	Genotyping (128)[d]	Sourc[e]
SJLB770	79.0	M	AA	√	√	√	√		SJ
SJLB773	47.0	F	C	√	√	√	√		SJ
SJLB774	58.0	F	C	√	√	√	√		SJ
SJLB779	47.0	F	C	√	√	√	√		SJ
SJLB780	70.0	M	C	√	√	√	√		SJ
SJLB782	59.0	M	U	√	√	√	√		SJ
SJLB786	16.0	M	C	√	√	√	√		SJ
SJLB792	59.0	M	C	√	√	√	√		SJ
SJLB793	36.0	F	C	√	√	√	√		SJ
SJLB794	16.0	M	C	√	√	√	√		SJ
SJLB795	50.0	M	C	√	√		√		SJ

Sample ID[a]	Age (year)	Sex[b]	Ethnicity[c]	Activity (n=333)	Proteomics (n=455)	mRNA expression (n=230)	Gene sequencing (n=296)[d]	Genotyping (128)[d]	Sourc[e]
SJLB797	12.0	F	C		√	√	√		SJ
SJLB798	64.0	M	C		√	√	√		SJ
SJLB81	52.0	M	C	√	√		√		SJ
SJLB837	40.0	F	C	√	√	√	√		SJ
SJLB845	10.0	F	C		√				SJ
SJLB848	53.0	M	C		√	√	√		SJ
SJLB849	46.0	F	C		√	√	√		SJ
SJLB85	67.0	F	C		√				SJ
SJLB856	67.0	M	C	√	√				SJ
SJLB860	47.0	M	C	√	√	√	√		SJ
SJLB864	21.0	F	C	√	√	√	√		SJ

Sample ID[a]	Age (year)	Sex[b]	Ethnicity[c]	Activity (n=333)	Proteomics (n=455)	mRNA expression (n=230)	Gene sequencing (n=296)[d]	Genotyping (128)[d]	Sourc[e]
SJLB865	34.0	M	C	√	√	√	√		SJ
SJLB867	30.0	M	C	√	√	√	√		SJ
SJLB888	58.0	F	C	√	√		√		SJ
SJLB898	28.0	F	C	√	√	√	√		SJ
SJLB900	49.0	M	C		√	√	√		SJ
SJLB903	41.0	U	C		√	√	√		SJ
SJLB904	80.0	F	C	√	√		√		SJ
SJLB905	87.0	F	C	√	√		√		SJ
SJLB908	68.0	M	C		√		√		SJ
SJLB913	69.0	F	C	√	√	√	√		SJ
SJLB921	50.0	F	C	√	√	√	√		SJ

Sample ID[a]	Age (year)	Sex[b]	Ethnicity[c]	Activity (n=333)	Proteomics (n=455)	mRNA expression (n=230)	Gene sequencing (n=296)[d]	Genotyping (128)[d]	Sourc[e]
SJLB923	68.0	M	C		√	√	√		SJ
SJLB932	62.0	M	C	√	√	√	√		SJ
SJLB934	45.0	M	C	√	√	√	√		SJ
SJLB938	8.0	M	C	√	√	√	√		SJ
SJLB939	24.0	M	C	√	√	√	√		SJ
SJLB943	56.0	F	C	√	√	√	√		SJ
SJLB944	77.0	F	C	√	√	√	√		SJ
SJLB947	45.0	F	C		√	√	√		SJ
SJLB948	50.0	M	C		√	√	√		SJ
SJLB949	42.0	F	C		√	√	√		SJ
SJLB951	53.0	F	C		√	√	√		SJ

Sample ID[a]	Age (year)	Sex[b]	Ethnicity[c]	Activity (n=333)	Proteomics (n=455)	mRNA expression (n=230)	Gene sequencing (n=296)[d]	Genotyping (128)[d]	Sourc[e]
SJLB955	68.0	F	C	√	√	√	√		SJ
SJLB956	52.0	F	C	√	√	√	√		SJ
SJLB959	71.0	F	C		√	√	√		SJ
SJLB96	63.0	M	C		√				SJ
SJLB961	80.0	F	C	√	√	√	√		SJ
SJLB962	63.0	F	C	√	√	√	√		SJ
SJLB963	60.0	F	C	√	√	√	√		SJ
SJLB964	70.0	F	C	√	√	√	√		SJ
SJLB965	24.0	F	C	√	√		√		SJ
SJLB967	57.0	M	C	√	√	√	√		SJ
SJLB968	61.0	M	C		√	√	√		SJ

Sample ID[a]	Age (year)	Sex[b]	Ethnicity[c]	Activity (n=333)	Proteomics (n=455)	mRNA expression (n=230)	Gene sequencing (n=296)[d]	Genotyping (128)[d]	Sourc[e]
SJLB969	50.0	M	C		√	√	√		SJ
SJLB972	73.0	M	C	√	√		√		SJ
SJLB979	20.0	M	C	√	√		√		SJ
SJLB980	44.0	M	C	√	√	√	√		SJ
SJLB981	62.0	F	C	√	√	√	√		SJ
SJLB990	80.0	M	U	√	√	√	√		SJ

[a] These samples are well characterized for the abundance or activity of various other enzymes and drug transporters previously (Paine et al., 1997; Dai et al., 2006; Hashizume et al., 2008; Naraharisetti et al., 2010; Deo et al., 2012; Edson et al., 2013; Prasad et al., 2013; Prasad et al., 2014; Wang et al., 2015; Pearce et al., 2016; Shirasaka et al., 2016; Bhatt et al., 2017; Boberg et al., 2017; Tanner et al., 2017; Xu et al., 2017; Billington et al., 2018; Wong et al., 2018).

[b] M: male; F: female; U: unknown

[c] C: Caucasian; AA: African American; His: Hispanic; PI: Pacific Islander; NA: Native American; U: unknown

[d] Gene sequencing is a method of determining genomic variations in a sample in relation to a common reference sequence whereas genotyping refers to the analysis of a targeted list of SNPs in the samples.

[e] CMKC: Children's Mercy Kansas City, MO; UW: University of Washington, Seattle, WA; SJ: St. Jude Children's Research Hospital, Miami, FL

√ symbol indicates available data.

Table S2. *UGT2B17 and UGT2B15* variants identified in the adult samples with allele frequency of >10%.

Protein name	Chromosome position	Nucleotide change	Amino acid change	rs Number	MAF	Significance association with mRNA expression or protein abundance or activity
UGT2B17	69415555	C>T	Intron	rs7436962	0.38	Yes (all)
	69415607	A>C	Intron	rs9996186	0.38	Yes (all)
	69417570	G>A	Synonymous	rs28374627	0.33	Yes (all)
	69420232	A>G	Intron	rs4860305	0.34	Yes (all)
UGT2B15	69536084	A>C	D85Y	rs1902023	0.48	Yes (activity)

Table S3: LC-MS/MS parameters for analysis of peptides.

LC gradient program						
Time (min)	Flow Rate	A (Water with 0.1% formic acid, %)		B (Acetonitrile with 0.1% formic acid, %)		
0	0.3	97		3		
4	0.3	97		3		
8	0.3	87		13		
18	0.3	70		30		
20.5	0.3	65		35		
21.1	0.3	40		60		
23.1	0.3	20		80		
23.2	0.3	97		3		
27	0.3	97		3		
MS Parameters						
Protein	Peptide sequence	Light/Heavy	Parent (*m/z*)	Daughter (*m/z*)	CE (eV)	DP (V)
CYP1A2	IGSTPVLVLSR	Light	571.4	783.5	73	29
			571.4	375.2	73	29
			571.4	392.3	73	29
		Heavy	576.4	793.5	73	29
			576.4	397.3	73	29
	YLPNPALQR	Light	536.3	277.2	80	19
			536.3	292.7	80	19
			536.3	303.2	80	19
			536.3	398.2	80	19
			536.3	584.4	80	19

		Heavy	536.3	795.5	80	19
			541.3	403.2	80	19
			541.3	594.4	80	19
			541.3	805.5	80	19
		Light	776.9	982.5	88	30
			776.9	867.5	88	30
	GTGGANIDPTFFLSR		776.9	522.3	88	30
		Heavy	781.9	992.5	88	30
			781.9	877.5	88	30
		Light	1204.6	1012.5	119	45
CYP2A6			1204.6	787.4	119	45
			1204.6	650.4	119	45
			1204.6	1147	119	45
	DPSFFSNPQDFNPQHFLNEK		1208.6	1020.5	119	45
		Heavy	1208.6	795.4	119	45
			1208.6	658.4	119	45
			1208.6	1151	119	45
		Light	605.3	648.4	80	22
			605.3	908.5	80	22
	TEAFIPFSLGK		605.3	979.6	80	22
		Heavy	609.3	656.4	80	22
CYP2B6			609.3	987.6	80	22
		Light	830.1	601.3	80	30
			830.1	665.3	80	30
	GIACHYLEEGAQCPAPLSYVPR		830.1	999.6	80	30
			830.1	831.5	80	30

CYP2C8	YSDLVPTGVPHAVTTDTK	Heavy	833.4	1009.6	80	30
			833.4	841.5	80	30
		Light	634.3	578.3	77	27
			634.3	711.9	77	27
			634.3	662.3	77	27
		Heavy	637	578.3	77	27
			637	666.4	77	27
CYP2C9	GIFPLAER	Light	451.8	293.2	64	17
			451.8	366.7	64	17
			451.8	585.3	64	17
			451.8	732.5	64	17
		Heavy	456.8	371.7	64	17
			456.8	595.3	64	17
	LPPGPTPLPVIGNILQIGIK	Light	1019.1	773.5	105	46
			1019.1	1068.7	105	46
			1019.1	962.6	105	46
			1019.1	914.1	105	46
		Heavy	1023.1	1076.7	105	46
			1023.1	918.1	105	46
			1023.1	773.5	105	46
			1023.1	966.6	105	46
CYP2E1	FITLVPSNLPHEATR	Light	848	574.4	93	39
			848	1121.6	93	39
			848	561.3	93	39
		Heavy	853	1131.6	93	39
			853	566.3	93	39

CYP2J2	FGPVFTLYVGSQR	Light	735.9	709.4	85	35
			735.9	447.2	85	35
			735.9	633.8	85	35
		Heavy	740.9	457.2	85	35
			740.9	638.9	85	35
	VIGQGQQPSTAAR	Light	656.9	915.5	79	33
			656.9	602.3	79	33
			656.9	550.8	79	33
		Heavy	661.9	612.3	79	33
			661.9	612.3	79	33
	LLDEVTYLEASK	Light	690.9	434.2	82	34
			690.9	710.4	82	34
			690.9	811.4	82	34
			690.9	910.5	82	34
			690.9	1154.6	82	34
		Heavy	694.9	819.4	82	34
			694.9	1162.6	82	34
CYP3A4	EVTNFLR	Light	439.7	229.1	63	25
			439.7	330.2	63	25
			439.7	650.4	63	25
		Heavy	444.7	229.1	63	25
			444.7	660.4	63	25
	LGIPGPTPLPFLGNILSYHK	Light	712.1	284.2	83	34
			712.1	846.5	83	34
			712.1	1044.6	83	34
			712.1	931.5	83	34

		Heavy	714.7	284.2	83	34
			714.7	846.5	83	34
			714.7	1052.6	83	34
			714.7	939.5	83	34
		Light	469.3	217.1	80	17
			469.3	234.2	80	17
	DTINFLSK		469.3	347.2	80	17
		Heavy	473.3	616.4	80	17
			473.3	729.4	80	17
		Light	896.5	741.4	97	34
			896.5	869.5	97	34
			896.5	1334.8	97	34
	LDTQGLLQPEKPIVLK		896.5	923.6	97	34
CYP3A5			896.5	569.4	97	34
		Heavy	900.5	931.6	97	34
			900.5	577.4	97	34
		Light	615.8	1016.6	76	24
			615.8	887.5	76	24
			615.8	774.5	76	24
	DVEINGVFIPK		615.8	504.3	76	24
			615.8	244.2	76	24
		Heavy	619.8	782.5	76	24
			619.8	252.2	76	24
		Light	695.4	262.1	82	30
CYP3A7	FNPLDPFVLSIK		695.4	803.5	82	30
			695.4	347.2	82	30

		Heavy	695.4	918.4	82	30
			699.4	262.1	82	30
			699.4	568.8	82	30
		Light	984.1	1331.7	103	44
			984.1	1121.6	103	44
	LGIPGPTPLPFLGNALSFR		984.1	764.4	103	44
			984.1	409.2	103	44
		Heavy	989.1	1131.6	103	44
			989.1	419.2	103	44
		Light	476.9	635.3	75	19
			476.9	734.3	75	19
CYP-reductase (POR)	FAVFGLGNK		476.9	488.3	75	19
		Heavy	480.8	643.4	75	19
			480.8	742.4	75	19
		Light	457.7	671.4	34	82
			457.7	260.2	34	82
			457.7	244.1	34	82
UGT1A1	DGAFYTLK		461.7	679.4	34	82
		Heavy K[13C6, 15N2]	461.7	268.2	34	82
			461.7	244.1	34	82
		Light	699.9	277.2	30	82
			699.9	364.2	30	82
UGT1A4	YLSIPAVFFWR		699.9	922.5	30	82
		Heavy R[13C6, 15N4]	704.9	277.2	30	82
			704.9	932.5	30	82
UGT1A6	DIVEVLSDR	Light	523.3	718.4	28	69

			523.3	589.3	28	69
			523.3	490.3	28	69
		Heavy R[13C6, 15N4]	528.3	728.4	28	69
			528.3	500.3	28	69
			320.2	444.2	15	55
		Light	320.2	370.7	15	55
UGT1A9	AFAHAQWK		320.2	335.2	15	55
		Heavy K[13C6, 15N2]	322.8	448.2	15	55
			322.8	374.7	15	55
			543.8	872.5	71	28
		Light	543.8	759.4	71	28
UGT2B4	TILDELVQR		543.8	644.4	71	28
		Heavy	548.8	882.5	71	28
			548.8	769.4	71	28
			550.8	886.5	29	71
		Light	550.8	773.4	29	71
			550.8	658.4	29	71
	TILDELIQR		550.8	416.3	29	71
			555.8	896.5	29	71
UGT2B7			555.8	783.4	29	71
		Heavy R[13C6, 15N4]	555.8	668.4	29	71
			555.8	426.3	29	71
			582.8	922.5	25	74
	IEIYPTSLTK	Light	582.8	809.4	25	74
			582.8	646.4	25	74

UGT2B15	SVINDPVYK	Heavy K[13C6, 15N2]	586.8	817.5	25	74
			586.8	654.4	25	74
		Light	517.8	424.7	69	23
			517.8	735.4	69	23
			517.8	848.5	69	23
		Heavy K[13C6, 15N2]	521.8	428.7	69	23
			521.8	856.5	69	23
UGT2B17	FSVGYTVEK	Light	515.3	795.4	27	69
			515.3	696.4	27	69
		Heavy K[13C6, 15N2]	519.3	704.4	27	69
			519.3	235.1	27	69
	SVINDPIYK	Light	524.8	862.5	23	69
			524.8	431.7	23	69
		Heavy K[13C6, 15N2]	528.8	870.5	23	69
			528.8	435.7	23	69
CES1	AGQLLSELFTNR	Light	674.9	257.1	33	80
			674.9	370.2	33	80
			674.9	866.4	33	80
		Heavy	679.9	257.1	33	80
			679.9	370.2	33	80
	EGYLQIGANTQAAQK	Light	796.4	350.1	31	89
			796.4	888.5	31	89
			796.4	417.2	31	89
		Heavy	800.4	350.1	31	89

CES2	ADHGDELPFVFR	Light	800.4	896.5	31	89
			701.8	1079.6	39	82
			701.8	665.4	39	82
			701.8	322.2	39	82
		Heavy	706.8	675.4	39	82
			706.8	332.2	39	82
	TTHTGQVLGSLVHVK	Light	788.9	739.4	37	89
			788.9	383.2	37	89
			788.9	687.9	37	89
		Heavy	793	391.3	37	89
			793	691.9	37	89
EPHX1	VETSDEEIHDLHQR	Light	427.7	403.2	62	25
			427.7	459.7	62	25
			427.7	689.8	62	25
		Heavy	430.2	408.2	62	25
			430.2	651.3	62	25
	YLEDGGLER	Light	526.3	277.2	70	28
			526.3	646.3	70	28
			526.3	775.4	70	28
		Heavy	531.3	277.2	70	28
			531.3	785.4	70	28
EPHX2	VCEAGGLFVNSPEEPSLSR	Light	1024.5	1115.5	106	50
			1024.5	914.5	106	50
			1024.5	559.3	106	50
		Heavy	1029.5	924.5	106	50
			1029.5	569.3	106	50

AOX1	ASPSEVVFLDDIGANLKPAR	Light	700.4	764.9	82	31
			700.4	715.4	82	31
			700.4	641.9	82	31
		Heavy	703.7	720.4	82	31
			703.7	769.9	82	31
	LILNEVSLLGSAPGGK	Light	784.5	886.5	88	42
			784.5	573.3	88	42
			784.5	358.2	88	42
		Heavy	788.5	581.3	88	42
			788.5	366.2	88	42
	GLHGPLTLNSPLTPEK	Light	837.5	1301.7	92	42
			837.5	1366.8	92	42
			837.5	1309.7	92	42
		Heavy	837.5	373.2	92	42
			841.5	1301.7	92	42
			841.5	1374.8	92	42
FMO3	NNLPTAISDWLYVK	Light	817.4	342.2	91	31
			817.4	1292.7	91	31
			817.4	646.8	91	31
		Heavy	821.4	342.2	91	31
			821.4	1300.7	91	31
	LVGPGQWPGAR	Light	569.3	400.2	73	25
			569.3	463.2	73	25
			569.3	434.7	73	25
		Heavy	574.3	410.2	73	25
			574.3	468.2	73	25

Bovine serum albumin (BSA)	AEFVEVTK	Light	461.8	722.4	26	70
			461.8	476.3	26	70
		Heavy K[13C6, 15N2]	465.8	730.4	26	70
			465.8	484.3	26	70
Human serum albumin (HSA)	LVNEVTEFAK	Light	575.3	694.4	30	80
			575.3	595.3	30	80
		Heavy K[13C6, 15N2]	579.3	702.4	30	80
			579.3	603.3	30	80
	VFDEFKPLVEEPQNLIK	Light	682.4	712.4	29	73
			682.4	970.5	29	73
		Heavy K[13C6, 15N2]	685.1	720.4	29	73
			685.1	978.5	29	73

Table S4: Validated LC-MS/MS method used for analysis of glucuronide metabolites (testosterone and DHT), and progesterone (internal standard).

LC gradient program (in vitro incubation for testosterone, DHT and progesterone)			
ACQUITY UPLC® BEH C18 column (2.1 × 50 mm, 1.7 µm)			
Time (min)	Flow rate (ml/min)	Water with 0.1% formic acid, %	Acetonitrile with 0.1% formic acid, %
0	0.25	97	3
0.5	0.25	97	3
2.0	0.25	45	55
3.2	0.25	20	80
3.4	0.25	20	80
3.5	0.25	97	3
5.0	0.25	97	3

MS Parameters				
Peptide type	**Parent ion (*m/z*)**	**Product ion (*m/z*)**	**CE (eV)**	**DP (V)**
Testosterone	289.2	97.1	30	80
		109.1	30	80
Testosterone - glucuronide	465.1	97.1	25	70
		109.1	25	70
DHT	291.4	255.2	28	106
		159.1	36	106
		91.1	84	106
		291.4	5	106
DHT- glucuronide	467.26	255.2	25	70
		159.1	31	70
		291.3	25	70
Progesterone (internal standard)	315.2	109.1	30	70
		97.1	30	70
Testosterone – glucuronide-d3	465.2	289.2	25	70
		271.2	30	70
DHT-glucuronide-d3	470.2	294.2	30	80
		276.2	30	80

Reanalysis (interday and intraday) of the quality control samples (i.e., standards spiked in the blank matrix) yielded consistent data (%CV < 5%). While progesterone was used as an internal standard for in vitro sample analysis, the quality of the chromatographic peaks of the analytes was confirmed by spiking labeled testosterone-glucuronide-d3 and DHT-glucuronide-d3 in the representative in vitro samples.

Table S5: Summary of Jonckheere-Terpstra test results (alternative hypothesis: two-sided)

	Covariate	J-T Statistic	P value
UGT2B17 mRNA abundance	• Diplotype (H1/H1 to H2/H2, all; Fig. 1D)	8131	1.32e-07
	• Diplotype (H1/H1 to H2/H2, male; Fig. 1D)	2431	0.000355
	• Diplotype (H1/H1 to H2/H2, female; Fig. 1D)	1117	7.032e-05
UGT2B17 abundance	• Diplotype (H1/H1 to H2/H2, all; Fig. 1E)	13788	8.958e-12
	• Diplotype (H1/H1 to H2/H2, male; Fig. 1E)	1395	9.108e-06
	• Diplotype (H1/H1 to H2/H2, female; Fig. 1E)	1248.5	5.96e-05
	• Age (neonatal - infant - early childhood- middle childhood- adolescence- adulthood; Fig. 2A)	18148	<2.2e-16
Testosterone-glucuronidation	• Diplotype (H1/H1 to H2/H2, all; Fig. 1F)	5004	5.775e-07
	• Diplotype (H1/H1 to H2/H2, male; Fig. 1F)	1197	0.0001934
	• Diplotype (H1/H1 to H2/H2, female; Fig. 1F)	695	7.399e-06
	• Age (neonatal - infant - early childhood- middle childhood- adolescence- adulthood; Fig 2E)	23964	<2.2e-16
DHT-glucuronidation	• Diplotype (H1/H1 to H2/H2, all; Fig. 1G)	4792	1.937e-05
	• Diplotype (H1/H1 to H2/H2, male; Fig. 1G)	1173	0.0005226
	• Diplotype (H1/H1 to H2/H2, female; Fig. 1G)	623	0.001602
	• Age (neonatal - infant - early childhood- middle childhood- adolescence- adulthood; Fig. 2I)	23363	2.309e-14

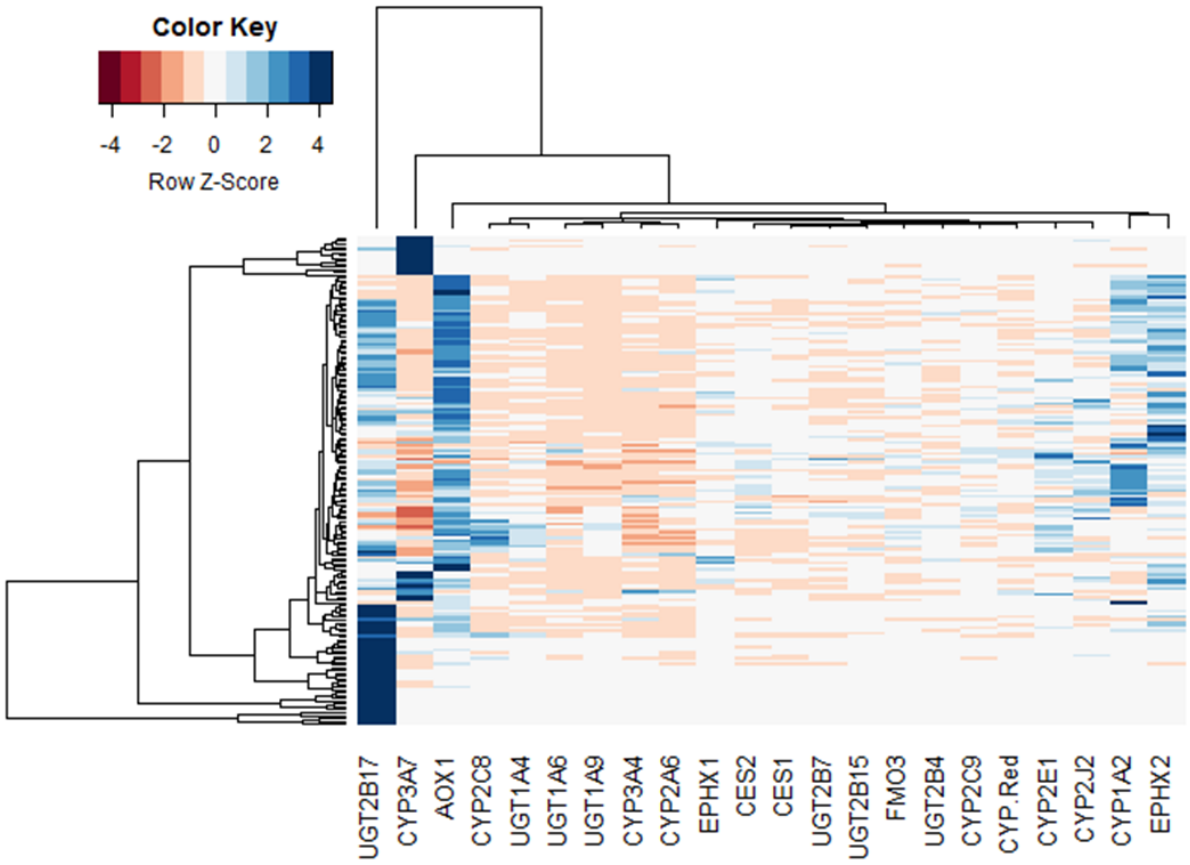

Figure S1. Hierarchical clustering of major drug metabolizing enzymes in human liver suggests unique protein abundance pattern for UGT2B17. Columns and rows indicate individual enzymes and individual samples (n=165), respectively. These data were the first set of analysis that included 128 pediatric and 37 adult samples (out of total 455).

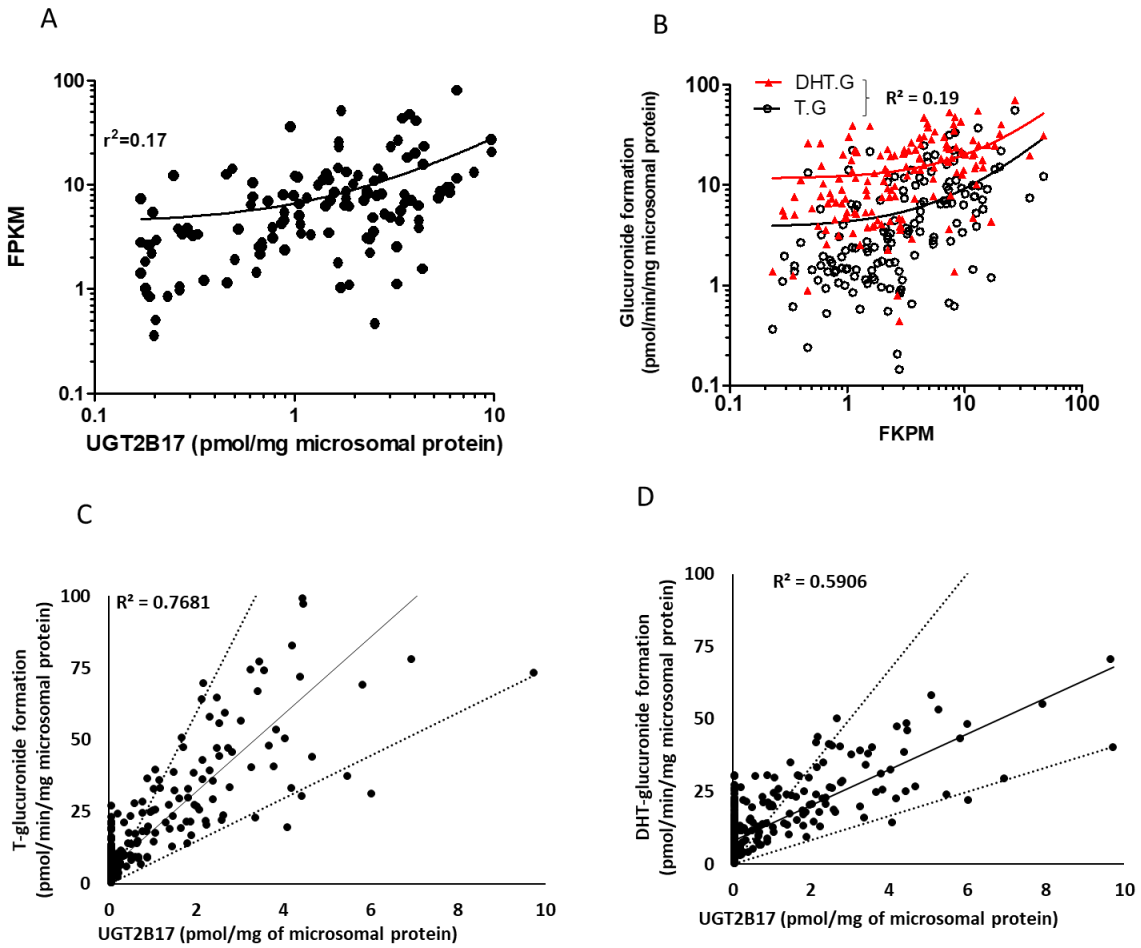

Supplementary Figure 2S. Correlation plot between UGT2B17 protein abundance and mRNA expression (A): Zero copy number and BLOQ samples were excluded from the mRNA-protein analysis. Correlation plot between UGT2B17 mRNA expression (FKPM) and T- and DHT-glucuronidation rates (B). UGT2B17 protein abundance is significantly associated with glucuronidation rates of T (C) and DHT (D) (n=346). Black dots represent data for individual subjects. Dotted trend-lines (in C and D) indicate two-fold range. FPKM-Fragments per kilobase of transcript per million mapped reads. T= Testosterone, DHT= Dihydrotestosterone.

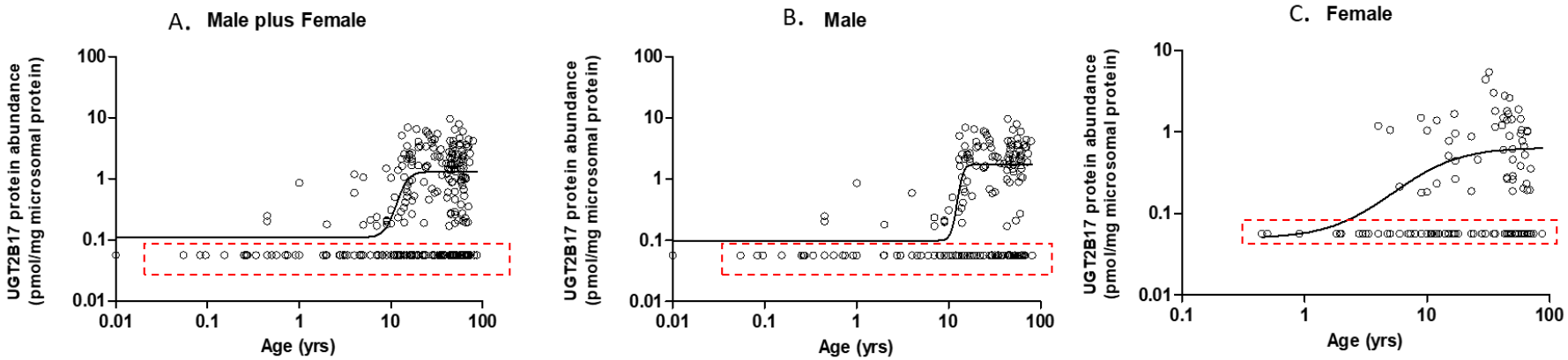

	Male plus female	Male	Female
Expression at birth (E_0) (pmol/mg of microsomal protein); Mean ± SE (95% CI)	0.11 ± 0.02 (0.1 to 0.2)	0.10 ± 0.02 (0.1 to 0.1)	0.05 ± 0.05 (0.0 to 0.1)
Adult_max expression (pmol/mg of microsomal protein); Mean ± SE (95% CI)	1.31 ± 0.15 (1.0 to 1.6)	1.75 ± 0.20 (1.3 to 2.2)	0.65 ± 0.18 (0.3 to 1.0)
Hill coefficient (h); Mean ± SE (95% CI)	7.5 ± 2.9 (1.7 to 13.3)	14.9 ± 6.4 (2.3 to 27.4)	1.8 ± 1.2 (0.0 to 4.2)
Age_{50} (years); Mean ± SE (95% CI)	13.5 ± 1.1 (11.3 to 15.8)	13.6 ± 0.6 (12.3 to 14.9)	10.7 ± 5.9 (<0 to 22.3)

Figure S3. Continuous age-dependent UGT2B17 protein abundance data in all (A), male (B) and female (C) donors. Donors carrying zero copy number were excluded from this analysis. 205 out of 375 of these samples (male plus females) were below the limit of quantification (BLOQ; enclosed by red-dotted squares). For statistical analysis, BLOQ samples were assigned a value of 0.057 pmol/mg of microsomal protein, which was 1/3rd of the lower limit of quantification (0.17 pmol/mg of microsomal protein). A non-linear, allosteric sigmoidal model (equation 1) was fitted to the continuous ontogeny protein abundance. In these samples, UGT2B17 was rarely (12 out of 92 samples) detected in children below age 9 years.

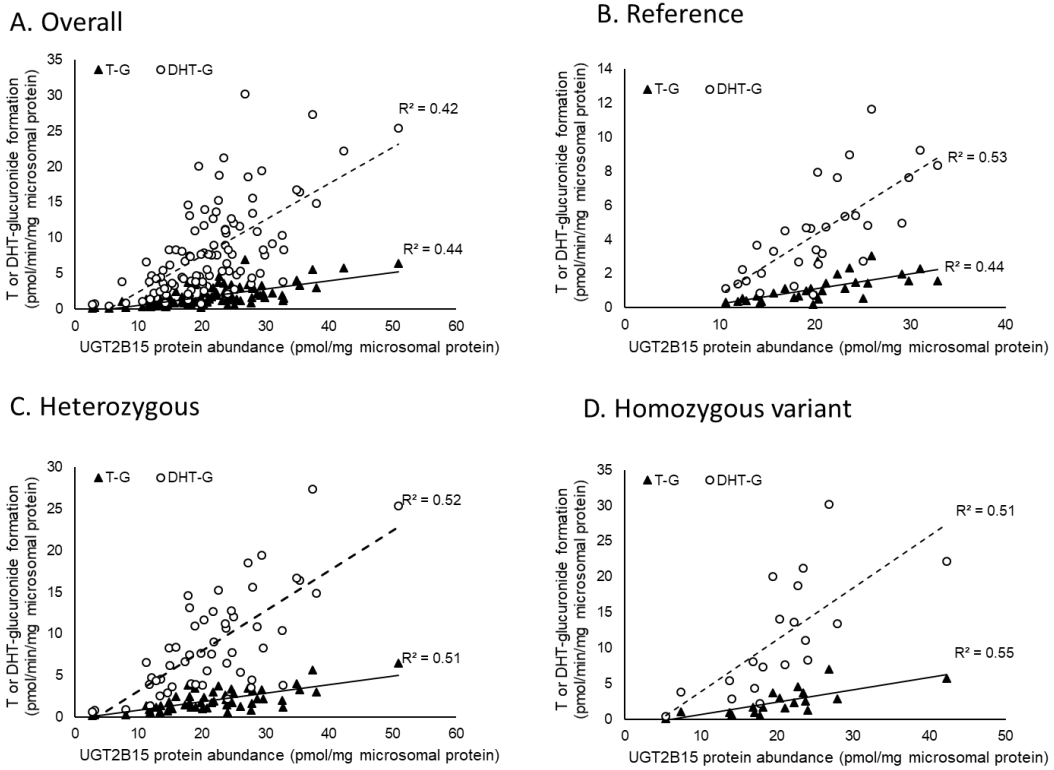

Figure S4. Effect of the *UGT2B15* SNP rs1902023 on testosterone- or DHT-glucuronide formation (pmol/min/mg microsomal protein), overall data set (A), reference (B), heterozygous (C) and homozygous variant (D) alleles. Only BLOQ (0.057 pmol/mg of microsomal protein) and zero copy number samples were included. testosterone-glucuronide, Testosterone-glucuronide and DHT-glucuronide, dihydrotestosterone glucuronide.

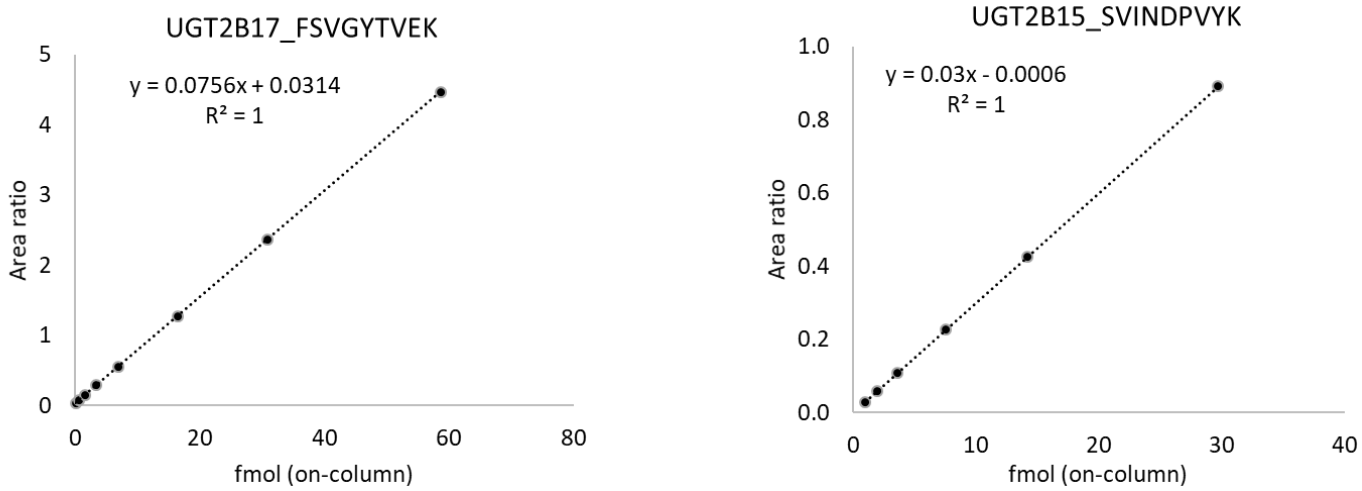

Figure S5. Calibration curve for UGT2B17 (0.10 to 58 fmol, on-column) and UGT2B15 (1.01 to 29.7 fmol, on-column) surrogate peptide standards.

References

Bhatt DK, Gaedigk A, Pearce RE, Leeder JS, and Prasad B (2017) Age-dependent Protein Abundance of Cytosolic Alcohol and Aldehyde Dehydrogenases in Human Liver. *Drug Metab Dispos* **45:**1044-1048.

Billington S, Ray AS, Salphati L, Xiao G, Chu X, Humphreys WG, Liao M, Lee CA, Mathias A, Hop C, Rowbottom C, Evers R, Lai Y, Kelly EJ, Prasad B, and Unadkat JD (2018) Transporter Expression in Noncancerous and Cancerous Liver Tissue from Donors with Hepatocellular Carcinoma and Chronic Hepatitis C Infection Quantified by LC-MS/MS Proteomics. *Drug Metab Dispos* **46:**189-196.

Boberg M, Vrana M, Mehrotra A, Pearce RE, Gaedigk A, Bhatt DK, Leeder JS, and Prasad B (2017) Age-Dependent Absolute Abundance of Hepatic Carboxylesterases (CES1 and CES2) by LC-MS/MS Proteomics: Application to PBPK Modeling of Oseltamivir In Vivo Pharmacokinetics in Infants. *Drug Metab Dispos* **45:**216-223.

Dai Y, Hebert MF, Isoherranen N, Davis CL, Marsh C, Shen DD, and Thummel KE (2006) Effect of CYP3A5 polymorphism on tacrolimus metabolic clearance in vitro. *Drug Metab Dispos* **34:**836-847.

Deo AK, Prasad B, Balogh L, Lai Y, and Unadkat JD (2012) Interindividual variability in hepatic expression of the multidrug resistance-associated protein 2 (MRP2/ABCC2): quantification by liquid chromatography/tandem mass spectrometry. *Drug Metab Dispos* **40:**852-855.

Edson KZ, Prasad B, Unadkat JD, Suhara Y, Okano T, Guengerich FP, and Rettie AE (2013) Cytochrome P450-Dependent Catabolism of Vitamin K: ω-Hydroxylation Catalyzed by Human CYP4F2 and CYP4F11. *Biochemistry* **52:**8276-8285.

Gaedigk A, Twist GP, and Leeder JS (2012) CYP2D6, SULT1A1 and UGT2B17 copy number variation: quantitative detection by multiplex PCR. *Pharmacogenomics* **13:**91-111.

Gordon AS, Fulton RS, Qin X, Mardis ER, Nickerson DA, and Scherer S (2016) PGRNseq: a targeted capture sequencing panel for pharmacogenetic research and implementation. *Pharmacogenetics and genomics*.

Hashizume T, Xu Y, Mohutsky MA, Alberts J, Hadden C, Kalhorn TF, Isoherranen N, Shuhart MC, and Thummel KE (2008) Identification of human UDP-glucuronosyltransferases catalyzing hepatic 1alpha,25-dihydroxyvitamin D3 conjugation. *Biochem Pharmacol* **75:**1240-1250.

Naraharisetti SB, Lin YS, Rieder MJ, Marciante KD, Psaty BM, Thummel KE, and Totah RA (2010) Human liver expression of CYP2C8: gender, age, and genotype effects. *Drug Metab Dispos* **38:**889-893.

Paine MF, Khalighi M, Fisher JM, Shen DD, Kunze KL, Marsh CL, Perkins JD, and Thummel KE (1997) Characterization of interintestinal and intraintestinal variations in human CYP3A-dependent metabolism. *The Journal of pharmacology and experimental therapeutics* **283:**1552-1562.

Pearce RE, Gaedigk R, Twist GP, Dai H, Riffel AK, Leeder JS, and Gaedigk A (2016) Developmental Expression of CYP2B6: A Comprehensive Analysis of mRNA Expression, Protein Content and Bupropion Hydroxylase Activity and the Impact of Genetic Variation. *Drug Metab Dispos* **44:**948-958.

Prasad B, Evers R, Gupta A, Hop C, Salphati L, Shukla S, Ambudkar SV, and Unadkat JD (2014) Interindividual Variability in Hepatic Organic Anion-Transporting Polypeptides and P-Glycoprotein (ABCB1) Protein Expression: Quantification by Liquid Chromatography Tandem Mass Spectroscopy and Influence of Genotype, Age, and Sex, in: *Drug Metab Dispos*, pp 78-88.

Prasad B, Lai Y, Lin Y, and Unadkat JD (2013) Interindividual variability in the hepatic expression of the

human breast cancer resistance protein (BCRP/ABCG2): effect of age, sex, and genotype. *J Pharm Sci* **102:**787-793.

Shirasaka Y, Chaudhry AS, McDonald M, Prasad B, Wong T, Calamia JC, Fohner A, Thornton TA, Isoherranen N, Unadkat JD, Rettie AE, Schuetz EG, and Thummel KE (2016) Interindividual variability of CYP2C19-catalyzed drug metabolism due to differences in gene diplotypes and cytochrome P450 oxidoreductase content. *Pharmacogenomics J* **16:**375-387.

Tanner J-A, Prasad B, Claw KG, Stapleton P, Chaudhry A, Schuetz EG, Thummel KE, and Tyndale RF (2017) Predictors of Variation in CYP2A6 mRNA, Protein, and Enzyme Activity in a Human Liver Bank: Influence of Genetic and Nongenetic Factors.

Vrana M, USA UoWDoPSW, Whittington D, Medicinal Chemistry UoWSWU, Nautiyal V, India IIoTKKWB, Prasad B, and USA UoWDoPSW (2017) Database of Optimized Proteomic Quantitative Methods for Human Drug Disposition‐Related Proteins for Applications in Physiologically Based Pharmacokinetic Modeling. *CPT: Pharmacometrics & Systems Pharmacology* **6:**267-276.

Wang L, Prasad B, Salphati L, Chu X, Gupta A, Hop CE, Evers R, and Unadkat JD (2015) Interspecies variability in expression of hepatobiliary transporters across human, dog, monkey, and rat as determined by quantitative proteomics. *Drug Metab Dispos* **43:**367-374.

Wong T, Wang Z, Chapron BD, Suzuki M, Claw KG, Gao C, Foti RS, Prasad B, Chapron A, Calamia J, Chaudhry A, Schuetz EG, Horst RL, Mao Q, Boer IHd, Thornton TA, and Thummel KE (2018) Polymorphic Human Sulfotransferase 2A1 Mediates the Formation of 25-Hydroxyvitamin D3-3-O-sulfate, A Major Circulating Vitamin D Metabolite in Humans.

Xu M, Bhatt DK, Yeung CK, Claw KG, Chaudhry AS, Gaedigk A, Pearce RE, Broeckel U, Gaedigk R, Nickerson D, Schuetz E, Rettie AE, Leeder S, Thummel KE, and Prasad B (2017) Genetic and Non-genetic Factors Associated with Protein Abundance of Flavin-containing Monooxygenase 3 in Human Liver. *The Journal of pharmacology and experimental therapeutics* **10.1124/jpet.117.243113**.